

# From Molecules to Systems: Sol–Gel Microencapsulation in Silica-Based Materials

Rosaria Ciriminna,<sup>†</sup> Marzia Sciortino,<sup>†</sup> Giuseppe Alonzo,<sup>‡</sup> Aster de Schrijver,<sup>§</sup> and Mario Pagliaro<sup>\*,†</sup>

Istituto per lo Studio dei Materiali Nanostrutturati, CNR, via U. La Malfa 153, 90146 Palermo, Italy, Dipartimento di Ingegneria e Tecnologie Agro Forestali, Università degli Studi, viale delle Scienze 13, 90128 Palermo, Italy, and Greenseal Chemicals NV, Port of Ghent, Haven 2270, Belgicastraat 3, B 9042 Gent, Belgium

Received May 28, 2010

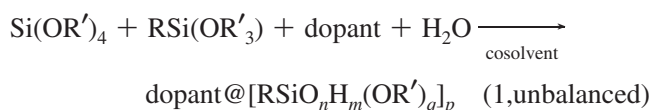
## Contents

1. Introduction	765
2. Principles	767
2.1. Silica Microparticles from W/O Emulsions	768
2.1.1. Hollow Spheres from W/O Microemulsions	770
2.2. Silica Microparticles from O/W Emulsions	772
2.2.1. Uniform Particles from O/W Emulsions	774
2.2.2. Microparticles from Emulsions with no Surfactant	774
2.2.3. ORMOSIL Nanoparticles from O/W Emulsions	777
2.3. Controlled Release	777
3. Applications	779
3.1. Advanced Sunscreens	780
3.2. Advanced Anti-Acne Therapy	781
3.3. Long-Lasting Yeast	782
3.4. Enhanced Insulating Materials	782
3.5. Self-Healing Cement	784
4. Economic and Environmental Considerations	785
5. Perspectives and Conclusions	787
6. Acknowledgments	787
7. References	788



Rosaria Ciriminna is a research chemist at Palermo's CNR Institute of nanostructured materials. Her interests span from catalysis and green chemistry to natural products, sol–gel materials, and supercritical carbon dioxide as an alternative reaction solvent. She has coauthored more than 60 research papers on these topics and was speaker at numerous international meetings. She started her career at Palermo's University in the late 1980s, working on the chemistry of natural products; in 1999 she began work on sol–gel catalysts for fine-chemicals synthesis. Her work has resulted in numerous achievements, including the recent commercialization of a Ru-based hybrid sol–gel catalyst for highly selective aerobic oxidations. Rosaria has also worked with Joël Moreau and Michel Wong at Montpellier's ENSCM and at the University of Reading in the U.K.

the dopant molecules at the onset of the sol–gel process (1):<sup>3</sup>



The silica cages provide chemical and physical stabilization of the entrapped dopant,<sup>4</sup> whereas the excellent physical properties of glass, such as optical transparency and permeability, allow applications that actually span all fields (analytical and synthetic) of chemistry and include optics and the functionalization of widely different materials, from textiles to construction materials.<sup>5</sup>

Equation 1 shows that the sol–gel process normally begins from molecular precursors and that it is possible to prepare a broad range of organically modified silicate systems (ORMOSILs)<sup>6</sup> by mixing more than one precursor. Research has shown that using this approach it is possible to repro-

## 1. Introduction

In 1984 Avnir and co-workers published the original paper<sup>1</sup> that demonstrated the feasibility of the concept of carrying out organic chemistry within the inner porosity of the inorganic material *par excellence*: glass, namely amorphous SiO<sub>2</sub>. It soon turned out that the approach to utilize molecules via structural organization in the solid state framework of porous silica could be extended to the large, delicate molecules of biochemistry, opening the route to practical applications of biotechnology.<sup>2</sup> In practice, organic molecules are entrapped in the inner porosity of a silica-based matrix used as parent material by simple addition of

\* To whom correspondence should be addressed. E-mail: mario.pagliaro@cnr.it.

<sup>†</sup> Istituto per lo Studio dei Materiali Nanostrutturati, CNR.

<sup>‡</sup> Università degli Studi.

<sup>§</sup> Greenseal Chemicals NV.



Marzia Sciortino is currently a Ph.D. student at the University of Palermo, Department of Agro-forest Engineering and Technologies. Her work, carried out also at Palermo's Institute of nanostructured materials, aims at the development of new silica-based microparticles for catalytic and cosmetic applications. In 2009 she was at Southern Illinois University (Carbondale, USA) working in the laboratories of Professor Bakul Dave. Prior to that, in 2008, Marzia graduated *cum laude* in pharmaceutical chemistry at the University of Palermo with a thesis on new polymeric micelles for drug delivery.



Giuseppe Alonzo holds the chair of inorganic chemistry at Palermo's University Agricultural Faculty. His current research at the Department of "Ingegneria e Tecnologie Agro Forestali" focuses on fast field cycling NMR studies of natural substances, including cellulose and other polysaccharides. Born in Palermo in 1946, he earned his master degree ("Laurea") in chemistry from the University of Palermo in 1971 under the supervision of Professor Nuccio Bertazzi. He began his academic career at the medical school of Palermo University in 1973. In 1975 and in 1983 he worked on tin complexes at Rutgers University with Professor Rolfe Herber. He then moved to the Agricultural Faculty of the University of Palermo, where he became full professor of inorganic chemistry in 1994. Professor Alonzo has coauthored some 120 publications and two chemistry textbooks for undergraduate students.

ducibly introduce the desired physical, mechanical, and functional properties in a modular fashion, opening the route to new functional materials that, ultimately, are designed from a molecular perspective.<sup>7</sup>

Microencapsulation, in its turn, is a hot topic in contemporary chemical research,<sup>8</sup> reflecting the increasing interest of chemical companies in the development of innovative "system solutions",<sup>9</sup> namely new functional materials in which known molecules are integrated to show new effects.

Enabling controlled release of a chemical, microencapsulation is useful for incorporating and isolating molecules that would not work without encapsulation, eliminate a processing step, and use more efficiently costly ingredients. In other words, this technology is mainly used for the purpose of protection and controlled release.<sup>10</sup>



Aster de Schrijver is director and shareholder of Altachem NV, a company specializing in the manufacture of special aerosol valves for viscous products and polyurethane foam applicator guns, and he is vice chairman of Tianrong Building Elements Company Ltd, China, a company producing sandwich panels filled with PU foam for buildings. Through his holding company FDS Invest ([www.fdsinvest.com](http://www.fdsinvest.com)) he has recently established also Greenseal Chemicals NV in Belgium and Greenseal Research Ltd in Portugal, two companies set up to develop and produce from "Greenfoam chemicals" to PU foam producers in aerosol cans and pressure vessels. Born at Bachte-Maria-Leerne (Belgium) in 1943, Mr. De Schrijver graduated as a chemical engineer from the University of Ghent (1969) and holds an MBA from the University of Antwerp (1982). He was invited speaker at numerous conferences on polyurethane foams in China, USA, and Europe, a topic on which he has authored two books. He started his career at the Belgian Shell Corporation Brussels (1969–1971) prior to join Imperial Chemical Industries from 1971–1975, where he was responsible for the development on rigid polyurethane foams. There he coined one component PU foams packed in pressure vessels, later sold for the first time in aerosol cans. Between 1975 and 1979 he joined Miczka Group, Germany, wherein as vice president he started up the first manufacturing companies to produce one component PU foams in aerosol cans in Germany, Switzerland, and the USA. Since 1981, he has been Chevalier de l'Ordre de la Couronne.

As put by Gosh,<sup>11</sup> microencapsulation is a process of enclosing micrometer-sized particles of solids or droplets of liquids or gases in an inert shell, which in turn isolates and protects them from the external environment. In general, two basic groups of microencapsulation techniques exist, namely chemical and physical (with the latter being divided into physicochemical and physicomechanical methods). *In-situ* processes such as emulsion, suspension, precipitation, or dispersion polymerization and interfacial polycondensations are the most important microencapsulation chemical techniques, whereas spinning-disk and spray-drying are the main physical methodologies.

The polymer phase separation technique known as coacervation—that is, partial desolvation of a homogeneous polymer solution into a polymer-rich phase that spontaneously deposits itself as a coating around the dispersed ingredient—and sol–gel microencapsulation are classified by Gosh as physicochemical techniques. Both have found a number of commercial applications. Currently, traditional low-volume markets for microcapsule-based products are expanding to include fine chemicals, adhesives, inks, fragrances, toners, sealants, and detergent manufacturers.<sup>12</sup> Offering competing technologies, microencapsulation companies include chemical makers, flavor and fragrance houses, and specialist firms.

In general, microcapsules may have regular or irregular shapes and, based on their morphology, which depends the deposition process of the shell as well as on the core material,



Mario Pagliaro currently leads Sicily's Photovoltaics Research Pole and a research Group at Italy's Research Council based in Palermo. His research interests are in sol–gel materials, glycerol's chemistry, solar energy, sustainability, science methodology, and management. His work has resulted in the joint development of several new chemical technologies, including some of the catalysts of the *SiliaCat* series, new biomass-based concrete additives, and oxygen sensors. Mario is the author of a large body of research papers as well as of scientific and management books. He regularly organizes conferences and gives courses, seminars, and tutorials on the topics of his research. In 2009 he chaired the 10th edition of FIGIPAS Meeting in Inorganic Chemistry, held in Palermo; in 2008 he gave the “John van Geuns” Lecture at the University of Amsterdam, and in 2005 he was appointed “Maître de conférences associé” at Montpellier's Ecole Nationale Supérieure de Chimie. He received his doctorate and master degrees from the University of Palermo following work carried out with David Avnir at the Hebrew University in Jerusalem and Arjan de Nooy at the TNO Food Research Institute in Zeist. He has also worked with Carsten Bolm at Aachen's Polytechnic and currently collaborates with 10 research groups in Italy and abroad.

they are classified as matrix, mononuclear, and polynuclear types (Figure 1).

In 2004, a study<sup>8</sup> aiming to identify trends in microencapsulation technologies since 1955 showed that liposome entrapment and spinning-disk were the dominant approaches; with nanoencapsulation growing but still far from the mainstream method. Among said nanoencapsulation approaches, sol–gel microencapsulation in silica-based materials is an emerging technology. This situation has not changed in the five subsequent years. Indeed, Figure 2 shows that only when the word “microsphere” is taken into account in the Boolean search using a scientific database (Scopus) does the number of papers published related to “sol–gel microencapsulation” exceed 600. In the latter case, furthermore, most of the papers published deal with encapsulation using long chain polymers as templates and do not mention removal of the templating polymers from the core of the resulting microspheres.

It may be concluded that sol–gel entrapment in silica-based microparticles is a relatively new solution for controlled release formulations despite the fact that, at least in principle, it offers a number of advantages over competing polymeric formulations.<sup>13</sup> For example, amorphous  $\text{SiO}_2$  is

a mechanically stable material which is also chemically and biologically inert<sup>14</sup> and thus compatible with most formulations of interest to medicine and cosmetics. Furthermore, organically modified silica microparticles share the versatility of organic polymers, with additional advantages enabled by the sol–gel process to tailor shape, density, amount, and surface properties of the resulting glassy materials.

In the simple and economical emulsion/sol–gel approach to organic–inorganic hybrid silicas of interest to this review, sol–gel molecular entrapment is carried out in or around emulsion droplets. Emulsions generally consist of two immiscible phases and are prepared by dispersing one liquid into another in the form of droplets, normally (but not always) in the presence of surface active material such as a surfactant.<sup>15</sup> Commonly used forms of emulsion are oil-in-water (O/W) and water-in-oil (W/O), as both can be stabilized and are useful in the synthesis of full or hollow particles. Two comprehensive reviews on the application of silica-based microparticles have been published, and both deal with the W/O emulsion approach. In one study,<sup>16</sup> Barbé and co-workers discuss how both the particle size and the release rate of silica-based microparticles can be tailored by controlling the processing conditions, whereas in a previous account<sup>17</sup> the same scientists reviewed sol–gel microencapsulation of bioactive molecules for drug-delivery in comparison with alternative systems.

However, there are no review articles covering microparticles obtained from oil-in-water (O/W) emulsions, despite the fact that these materials were the first to find commercial applications in cosmetics and in medicine, where water-based products or emulsions with an external water phase are preferred over oil-based products (ointments) or water-in-oil emulsions.

Referring to numerous achievements as well as to selected practical applications, we show in this account how doped microparticles with novel structural and functional responses are effectively designed using a molecular chemistry approach in which the parameters of the sol–gel/emulsion process are selected to ensure effective performance of the resulting microparticles in a number of applications in which silica-based microparticles behave as “smart” materials able to sense and respond to environmental stimuli in a useful manner. An effort was made to form a unified picture of this rapidly expanding field of nanochemistry based on the chemical principles behind the emulsion-based approaches, with the overall aim to provide guidelines to readers seeking new practical applications of sol–gel microparticles in their field of interest. The years of literature covered in this review include the first months of 2010 and go back to 1984, when the original Avnir and Reisfeld paper<sup>1</sup> mentioned in the *incipit* was published. The study ends with economic and environmental considerations that further support our argument that sol–gel microencapsulation will become one of the most relevant chemical technologies with applications in numerous industrial sectors.

## 2. Principles

Sol–gel microparticle formation is one case in which “soft matter” (lyotropic mesophases, foams, and emulsion; Scheme 1)<sup>18</sup> is used to template the resulting porous material in a basic chemical strategy for making functional nanomaterials that has been named by Ozin “nanochemistry”.<sup>19</sup>

In the case of sol–gel microparticles, the approach of interest to this account utilizes an interfacial polymerization

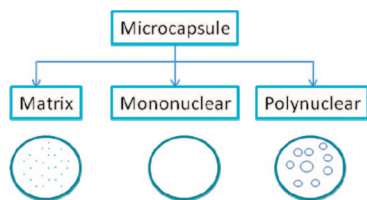


**Figure 1.** Morphology of microcapsules. (Adapted from ref 11).

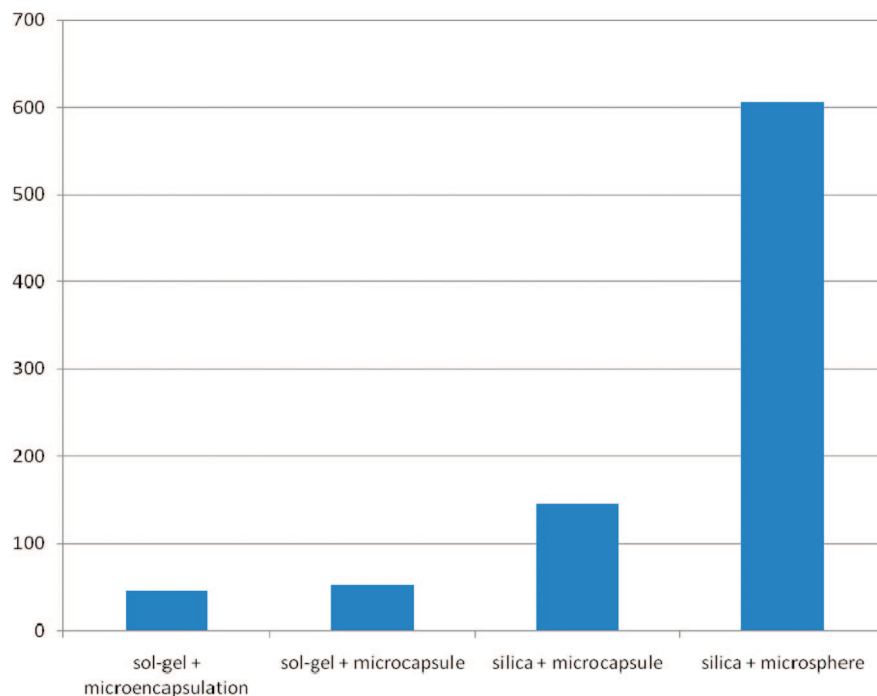
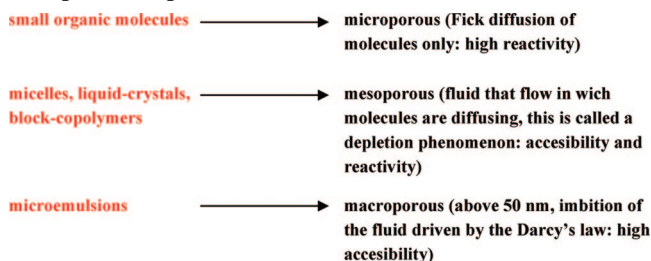


**Figure 2.** Number of papers published and patents related to “sol-gel microencapsulation”. The keywords used for the Boolean search are shown in the abscissa axis. (Date range, all years to May 1, 2010; Source, Scopus].

**Scheme 1. How Organic Templates Control Porosity of Materials (and Consequences from a Functional, Reactivity Viewpoint) [Reproduced from Ref 22 with Permission]**



process in which the mild sol–gel production of silica glass is combined with emulsion chemistry. In brief, the emulsion droplets provide a “microreactor” environment for the hydrolysis and condensation reactions of Si alkoxides.

In general, ionic and nonionic surfactants are widely exploited as structuring agents to make silica microparticles.<sup>20</sup> Ionic detergents, such as CTAB (cetyltrimethylammonium bromide) or SDS (sodium dodecyl sulfate), give pore sizes between 2 and 4 nm, whereas nonionic surfactants such as the Pluronics (a series of polyethylene oxide–polypropylene oxide triblock copolymers) and the Tween surfactant series (ethoxylated sorbitan esters) give materials with larger pores (around 10 nm) and thicker walls. We recall here that, in the case of both xerogels and microparticles, the molecular sol–gel encapsulation phenomenon results in pronounced physical and chemical protection deriving from the caging and isolation of the dopant molecule from its surroundings (Figure 3),<sup>4</sup> while the silica matrix offers better tightness and resistance to extraction forces than polymers or waxes.

In the case of fully dried gels, or xerogels, the interfacial structure of the nanoscopic sol–gel cage influences the reactivity of the entrapped reagents in a predictable manner so that functional materials with advanced chemical properties can be designed and fabricated.<sup>21</sup> In practice, beyond porosity that ensures accessibility and effective confinement

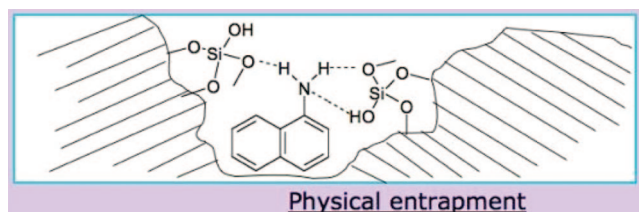


**Figure 3.** Physical entrapment of a dopant molecule in the inner porosity of a sol–gel silica matrix [Image courtesy of Prof. D. Avnir].

of the entrapped molecules, it is the morphology of sol–gel materials, both on the macro-, meso-, and nanoscale, that controls function and utility.<sup>22</sup>

The main reasons for opting for microparticles instead of xerogels then lie (i) in the far higher load of active ingredient that can be entrapped (up to 90% in weight of the final materials) as well as (ii) in the wide control over the release rate (from hours to months) thanks to control of the microstructure. Finally, (iii) silica microparticles in general show enhanced chemical stability even in corrosive environments (Figure 4).

Overall, therefore, sol–gel microparticle technology ensures an enhanced degree of encapsulation *and* better controlled release. As a result, all sorts of molecules can be entrapped and stabilized in ceramic microparticles with broad control over the release rate for a range of applications (such as drug delivery, release of specialty chemicals, and cosmeceutical/nutraceutical and beyond; Figure 5), with no need for reformulation for different molecules.

Before further exploration of the release properties of these systems, therefore, it is useful to review the two main techniques to prepare sol–gel microparticles, namely from water-in-oil (W/O) and from oil-in-water (O/W) emulsions.

## 2.1. Silica Microparticles from W/O Emulsions

Water-soluble molecules can be effectively entrapped in a number of silica-based ceramic particles with independent

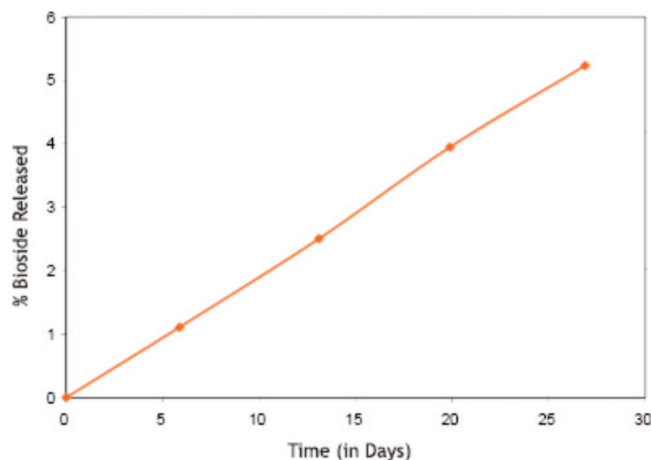


**Figure 4.** Slow release of a hydrophobic biocide, encapsulated in derivatized silica particles, into sodium hydroxide solution (pH = 12), demonstrating the stability of the particles to corrosive environments [Image courtesy of CeramiSphere Ltd.].

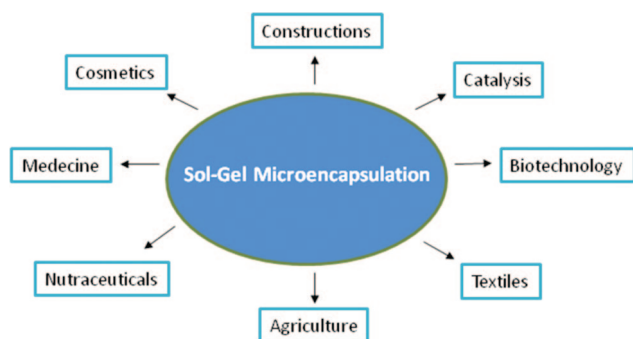


**Figure 5.** Potential application of sol–gel microparticles.

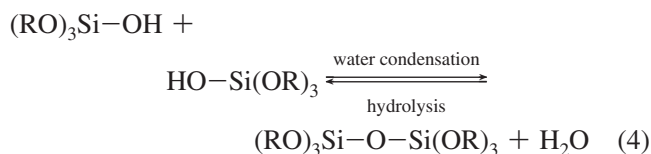
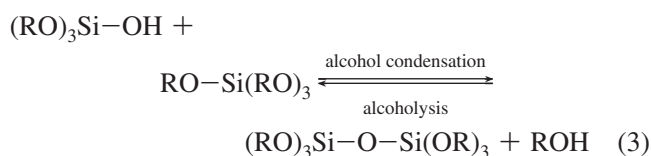
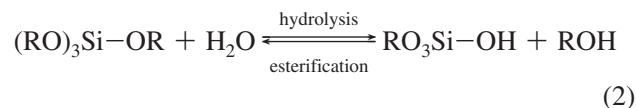
control over the release rate and particle size using reverse water-in-oil emulsions.<sup>15</sup> The active molecules are located in the aqueous droplets of an emulsion dispersed in a nonpolar solvent and stabilized by a surfactant. The process has been extensively explored by Barbé and co-workers in Australia (where the same scientists established the spin-off company CeramiSphere),<sup>23</sup> and can be viewed as an emulsification of a sol–gel solution in which gelation takes place concomitantly (Scheme 2).

Encapsulation occurs as the silicon precursors polymerize to build an oxide cage around the polar droplets which, acting as microreactors, yield microparticles with size comparable to the size of the droplets. The larger the amount of water employed, the larger the drops and thus the final microparticles. Hence, by changing the solvent–surfactant combination, namely the emulsion parameters, the particle size can be varied in the wide 10 nm–100 μm size range (Figure 6).<sup>16</sup> In detail, surfactants with HLB (hydrophile–lipophile balance) lesser than 10 (such as Span 80, with HLB = 4.3; or Span 20, with HLB = 8.6) are preferred for microsphere synthesis whereas surfactants with midrange HLB (between 10 and 15) are normally selected for nanoparticle synthesis. We remind here that the HLB number (a value between 0 and 60) defines the affinity of a surfactant for water or oil as it measures the ratio of hydrophilic and lipophilic groups in surfactant amphiphilic molecules.<sup>24</sup> HLB numbers > 10 point to an affinity for water (hydrophilic) whereas HLB values < 10 indicate affinity for oil (lipophilic).

Depending on the order of addition of the different chemicals, furthermore, the porous microparticles prepared from interfacial hydrolysis and condensation of TEOS in a

W/O emulsion will be full or hollow spheres (see below). Normally, if the emulsification of the sol–gel solution takes place concomitantly with gelation (Scheme 2), full (matrix) microparticles are formed with the dopant molecules homogeneously distributed within the inner huge porosity of the particles (typically, several hundred m<sup>2</sup>/g).

By changing the pH of the sol–gel solution, wide control of the size and shape of the silica polymers evolving at the water/oil interface is achieved. The rate of hydrolysis of Si(OR)<sub>4</sub> (eq 2) exhibits a minimum at pH 7 and increases exponentially at either lower or higher pH. In contrast, the rate of condensation (eqs 3 and 4) exhibits a minimum at pH 2 and a maximum around pH 7, where SiO<sub>2</sub> solubility and dissolution rates are maximized.<sup>13</sup>

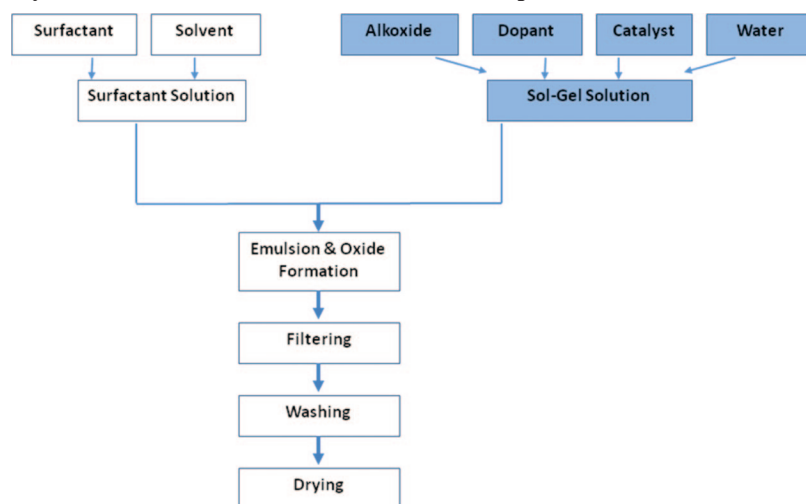


At low pH, acid catalysis promotes hydrolysis but hinders both condensation and dissolution reactions.<sup>25</sup> Consequently, for the microemulsion synthesis of silica particles using acid catalysis, small growth is observed and smaller, homogeneous particles are formed (Figure 7).<sup>26</sup>

This is shown by *in situ* FTIR measurements (Figure 8) that reveal that when introduced into the microemulsion, TMOS slowly diffuses into the water droplets of the reverse micelle, where it is hydrolyzed. Comparison between the intensity of the methanol ν(C–O) band at 1028 cm<sup>−1</sup> and the disappearing ν<sub>as</sub>SiO<sub>4</sub> bands at 843 and 825 cm<sup>−1</sup> under acidic and basic conditions shows that, after 2 min only, TMOS is 70% hydrolyzed in the microemulsion at pH 1.05, compared to 35% at pH 10.85. After 30 min, TMOS is completely hydrolyzed in the acid system but only 70% hydrolyzed in the basic solution, where even after 60 min a 10% fraction of TMOS is still unhydrolyzed.

Hydrolysis inside the water droplets of a water-in-oil microemulsion occurs more than an order of magnitude faster than that in typical single-phase sol–gel solution at the same concentration, as a result of the high *local* water concentration. Again, this is shown by *in situ* FTIR and by comparison of hydrolysis rates at pH 1.05 for the microemulsion and nonmicellar systems (Figures 8a and 9) with only 70% of TMOS hydrolyzed after 60 min in acetonitrile solution.

Under acidic conditions where hydrolysis is rapid and condensation is the rate-limiting step, the SAXS analysis of the evolving particles shows that the spheres formed are highly uniform, deriving from a relatively ordered micelle nanoparticle structure that exhibits sufficient long-range order to generate a peak in the scattering pattern at *q* = 0.05 Å<sup>−1</sup> (Figure 10).

**Scheme 2. Microparticles Synthesis Flow-Chart from W/O Emulsions [Reproduced from Ref 17 with Permission]**

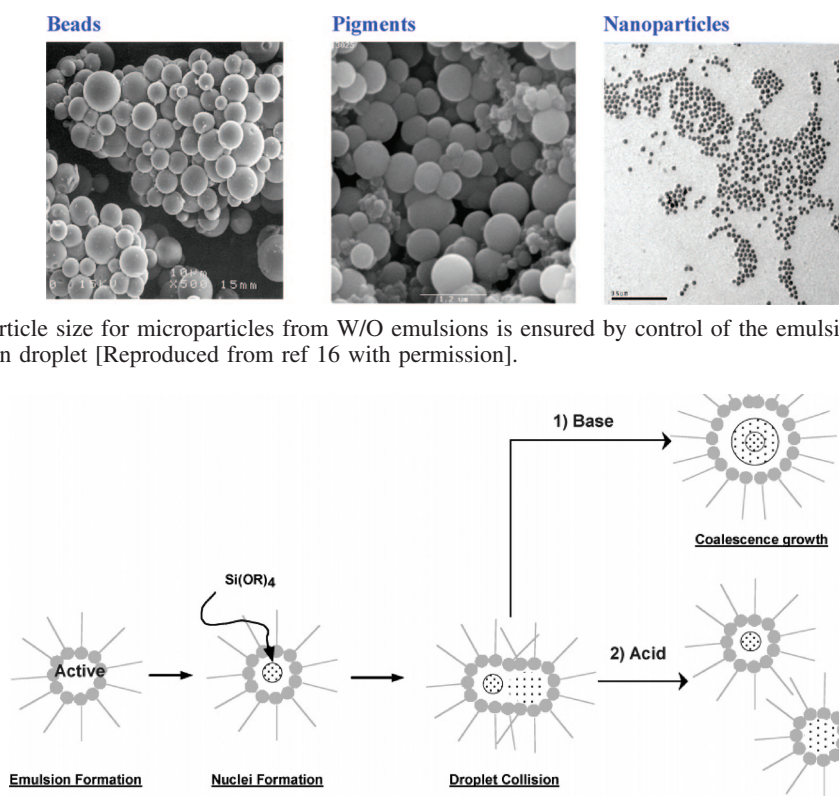
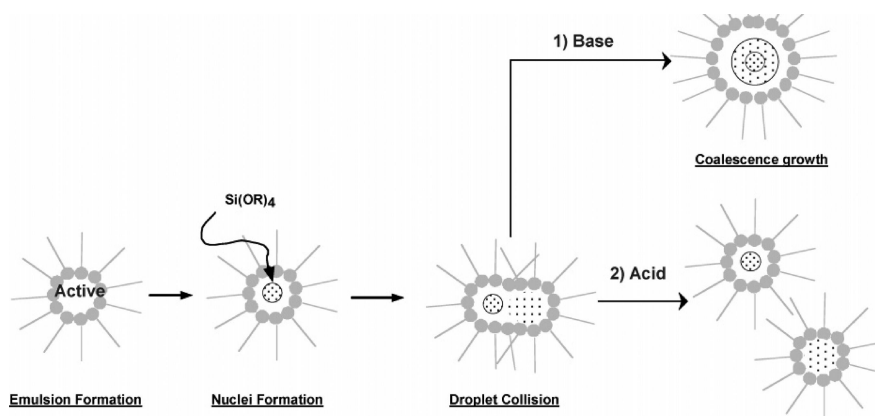
Base catalysis of sol–gel hydrolysis and condensation reactions, in contrast, promotes fast condensation and dissolution. This leads to the production of an inhomogeneous system due to rapid condensation of all the hydrolyzed precursor monomers and to the formation of dense silica particles by the ripening of aggregates formed during the collision of droplets (Figure 7).

As a result, the microparticles are dense; namely, their scattering length is that of amorphous silica, with essentially no porosity, with the particles being stabilized by a water/surfactant layer on the particle surface that prevents particle precipitation.<sup>25</sup> In other words, base-catalyzed microparticle synthesis in W/O microemulsions results in the formation of relatively large matrix particles of low and even negligible porosity. This result is of general validity. Thus, in order to obtain porous microcapsules under

base-catalyzed conditions, the “two-step” sol–gel polycondensation process<sup>27</sup> must be employed in which hydrolysis is first conducted under strong acidic conditions followed by condensation catalyzed by base. When this approach is adopted, large mesoporous microspheres can be synthesized also in basic W/O emulsions. In contrast, smaller particles synthesized in acid exhibit a strong microporous component (Figure 11).

### 2.1.1. Hollow Spheres from W/O Microemulsions

Hollow silica spheres (microcapsules) have a high dopant storage capacity because of their unique hollow core structures acting as a “molecular reservoir”; and they also have excellent sustained release properties (discussed later) which are ideal for drug release medical applications.

**Figure 6.** Tailored particle size for microparticles from W/O emulsions is ensured by control of the emulsion chemistry, which dictates the size of the emulsion droplet [Reproduced from ref 16 with permission].**Figure 7.** Proposed mechanism for particle formation under acidic and basic conditions [Reproduced from ref 26 with permission].

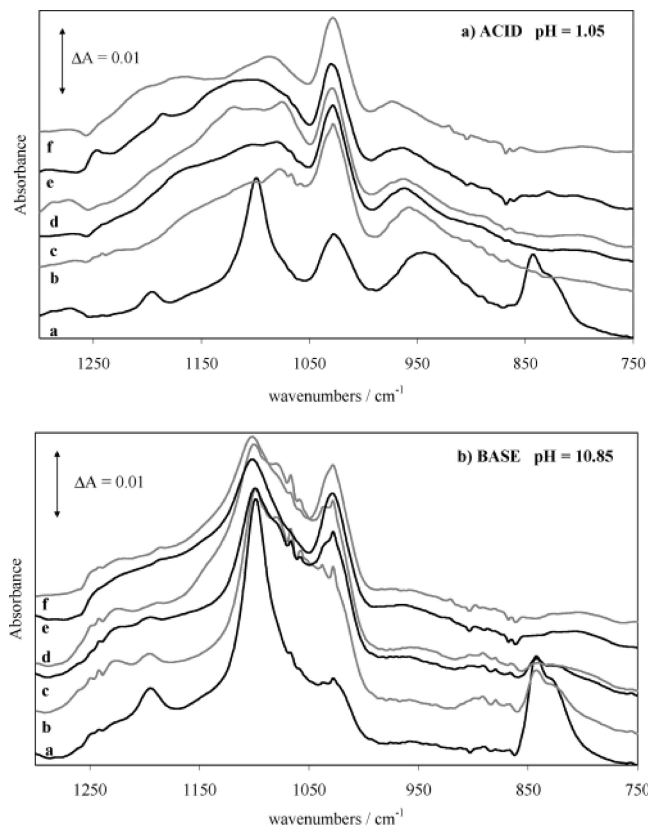


**Figure 8.** IR spectra ( $1300\text{--}750\text{ cm}^{-1}$ ) following TMOS addition to (a) acidic (pH 1.05) and (b) basic (pH 10.85) microemulsions after stirring for (a) 2, (b) 30, (c) 60, (d) 120, (e) 240, and (f) 360 min [Reproduced from ref 26 with permission].

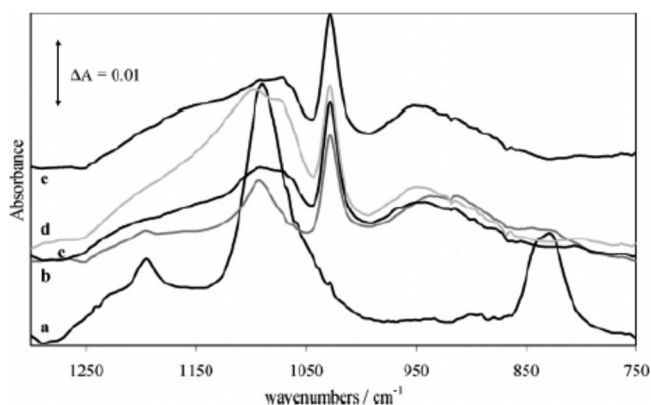


**Figure 9.** IR spectra ( $1300\text{--}750\text{ cm}^{-1}$ ) following TMOS reaction with dilute acid (pH 1.05) in acetonitrile after stirring for (a) 2, (b) 60, (c) 180, (d) 300, and (e) 360 min [Reproduced from ref 26 with permission].

For example, the direct encapsulation and storage of water-soluble molecules into silica microcapsules can be achieved using the water phase in a W/O emulsion as a container, forming an emulsion *prior* to addition of TEOS.<sup>28</sup> Now the Si alkoxide is introduced in the oil phase and slowly diffuses through the surfactant wall in the water droplets, where it is hydrolyzed and condensed, giving rise to gradual gelation of the stable microemulsion at the interface, with formation of microcapsules instead of full microparticles (Figure 12).

A typical preparation procedure used a drug aqueous solution obtained by dissolving 0.2 g of the drug (the antibiotic gentamicin sulfate) and 0.04 g of Tween 80 into 2 mL of 2 M HCl aqueous solution.<sup>27</sup> The resulting solution was added into 50 mL of cyclohexane solution containing

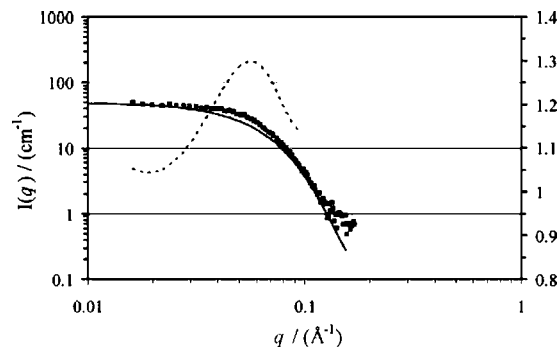


**Figure 10.** Apparent  $S(q)$  function (---) obtained by dividing SAXS of evolving silica particles in the acid-catalyzed system, 180 min after initiating hydrolysis (■), by the corresponding fitted  $P(q)$  [Reproduced from ref 26 with permission].

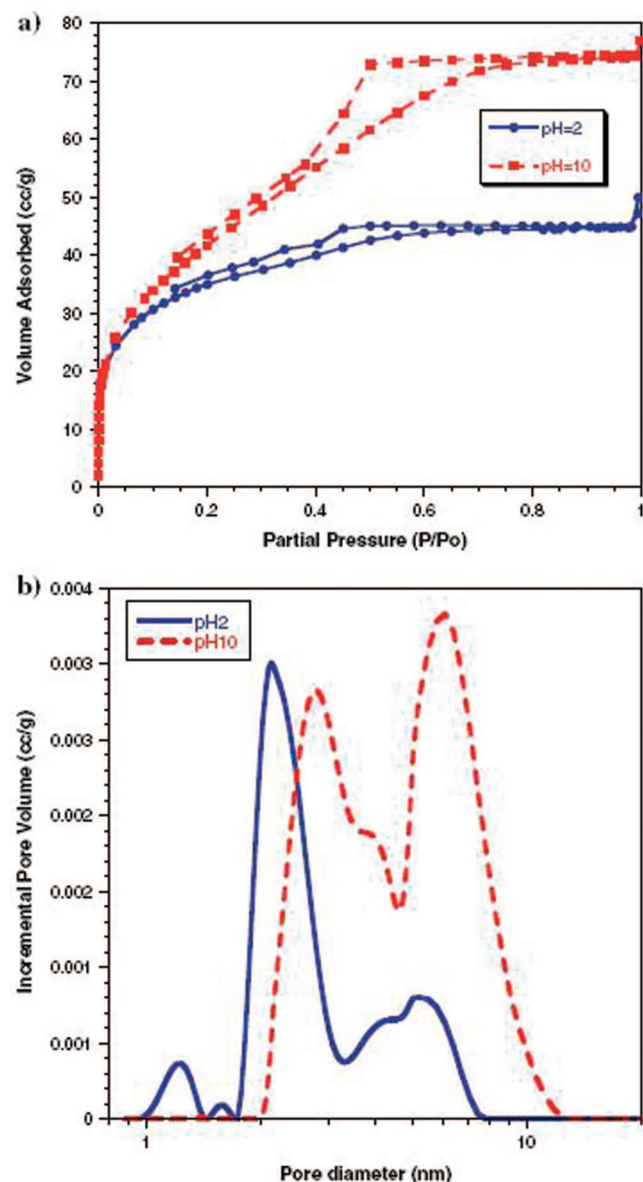


**Figure 11.** Adsorption isotherms (top) and pore size distribution for microparticles synthesized from W/O emulsions at acidic and basic pH [Reproduced from ref 16 with permission].

2.0 g of Span 80, and after vigorous agitation for 30 min, 1.865 mL of TEOS was added into the formed W/O emulsion with stirring for 24 h at room temperature. The solid was collected by filtration, washed with cyclohexane, and dried

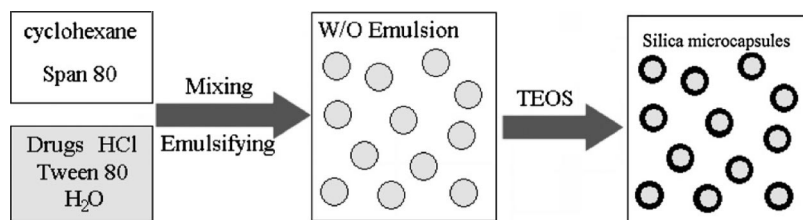


**Figure 12.** Schematic procedure for direct encapsulation of water-soluble drugs into silica microcapsules [Reproduced from ref 28 with permission].

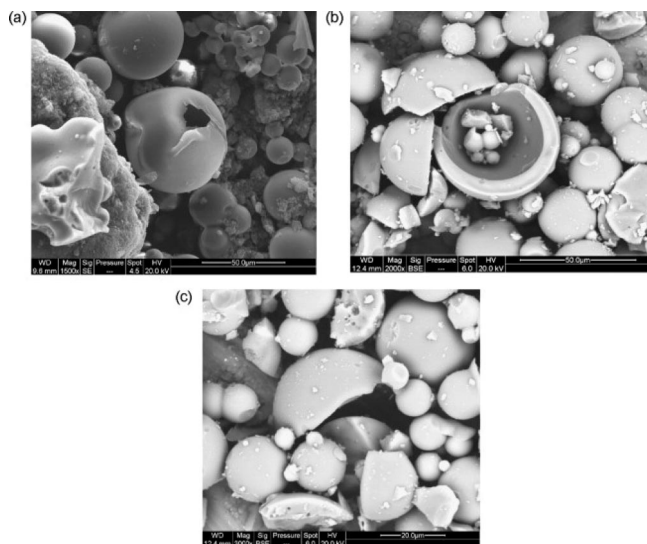


**Figure 13.** SEM micrographs of hollow silica microspheres: (a) densities less than  $1 \text{ g cm}^{-3}$  (calcined at  $500^\circ\text{C}$ ); (b) densities less than  $1 \text{ g cm}^{-3}$  (calcined at  $700^\circ\text{C}$ ); (c) densities less than  $1.74 \text{ g cm}^{-3}$  (calcined at  $700^\circ\text{C}$ ) [Reproduced from ref 29 with permission].

at  $40^\circ\text{C}$  for 2 h. Finally, silica microcapsules doped with gentamicin sulfate only were isolated after washing with ethanol to remove the residual surfactants and drying at  $40^\circ\text{C}$  overnight.

Also, the employment of ethanol as cosolvent in the W/O method affords completely hollow microparticles.<sup>29</sup> In this case, it is enough to carry out at  $80^\circ\text{C}$  the polycondensation in paraffin in the presence of the nonionic surfactant Span-80 of an acid sol containing ethanol ( $\text{TEOS}/\text{H}_2\text{O}/\text{EtOH} = 1:4:3$ ) prehydrolyzed at  $50^\circ\text{C}$ , to obtain  $\text{SiO}_2$  microcapsules whose shape and size is effectively controlled by the amount of TEOS and by the temperature of subsequent calcination (Figure 13).

Microspheres were subjected to density fractionation to determine the yield of hollow spheres. The sizes (outer diameters) of the spheres vary approximately between 5 and  $60 \mu\text{m}$ . The SEM pictures in Figure 13 show that the spheres (lightly crushed to examine the hollowness of the spheres), whose density is below  $1 \text{ g cm}^{-3}$ , are hollow, whereas the particles of densities approaching  $1.74 \text{ g cm}^{-3}$  (which is about 80% of the theoretical density of silica,  $2.24 \text{ g cm}^{-3}$ ) are full solid particles.

Hollowness of the spheres arises from the evaporation of water and ethanol from the core of spherical droplets. A decrease in calcination temperature also resulted in a full yield of hollow spheres with a 100% net yield of spheres of densities below  $1.74 \text{ g cm}^{-3}$ . This suggests that slower diffusion kinetics at lower calcination temperature is crucial in maximizing the yield of hollow spheres.

Stirring of the water-in-oil emulsion leads to the formation of sol droplets containing water and ethanol inside the

emulsion drop, protected by the adsorbed layer of Span-80 molecules (Figure 14). The nonpolar alkyl chains of TEOS molecules partly hydrolyzed preferably orient toward the outer periphery of the emulsion drop, i.e. toward the nonpolar paraffin oil. Therefore, hydrolysis and later condensation of hydrolyzed species to silica molecules takes place at the oil–drop interface, forming in the process a silica shell growing in thickness from the oil–drop interface toward the core of the drop.

Subsequent washing removes the oil and some surfactant, with the remaining surfactant at the interface (the as-synthesized particles are yellowish) evaporating during calcinations along with residual water and ethanol in the core.

## 2.2. Silica Microparticles from O/W Emulsions

Direct entrapment of hydrophobic molecules from W/O microemulsions is not possible and requires the use of multiple O/W/O<sup>30</sup> or W/O/W<sup>31</sup> emulsions to avoid rapid and complete migration of the lipophilic molecules in the oil phase. If a double emulsion is used, then liquid and solution hydrophobes can be incorporated in hollow microparticles in which the silica glass microcapsules formed by the interfacial polycondensation sol–gel process consist of a core of the entrapped dopant surrounded by a silica shell (Figure 15).

However, the technology best suited to simply encapsulate hydrophobic molecules such as essential oils, flavors, vitamins, proteins (including enzymes), and many other biomolecules makes use of an O/W emulsion, extending the approach first demonstrated by Takahashi and co-workers in 1998, for which cooperative assembly of silica and surfactants takes place at an oil–water interface, leading to hollow mesoporous silica spheres.<sup>32</sup> In detail, Takahashi reported that formation of spherical silica microcapsules (average diameter  $3.6 \mu\text{m}$ ) in O/W emulsions required a high water-to-surfactant molar ratio as well as fast agitation to ensure formation of oil droplets small enough to afford formation of homogeneous microparticles.

In 2001, therefore, Avnir and co-workers extended the method to comprise molecular encapsulation, demonstrating the broad scope of the O/W methodology to obtain doped microcapsules for diverse applications.<sup>33</sup> In the first step, a mixture containing the dopant, the water-insoluble Si alkoxides, and a surfactant is emulsified by stirring it in water. In the second step, amorphous  $\text{SiO}_2$  microcapsules are obtained by hydrolytic polycondensation in a water phase containing a surfactant catalyzed by base or acid, typically at temperatures in the  $50\text{--}70^\circ\text{C}$  range (Scheme 3).

The resulting particles typically have size values ranging between 0.3 and  $3 \mu\text{m}$  and a characteristic core–shell structure, with the dopant enclosed within the silica shell (Figure 16).

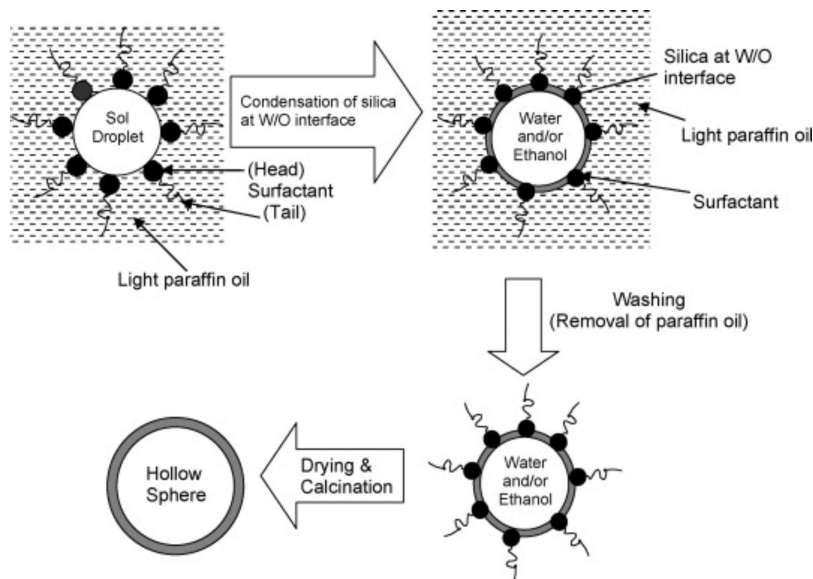
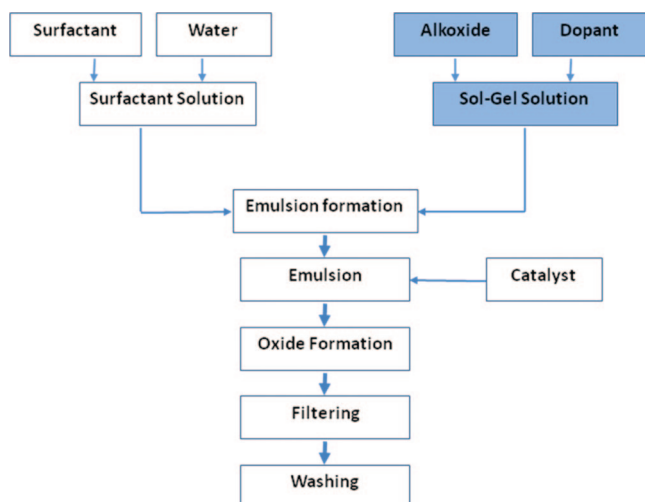


**Figure 14.** Schematic representation of the formation of hollow silica spheres [Reproduced from ref 29 with permission].



**Figure 15.** X-ray tomographic view of oil encapsulated inside pure silica microparticles [Image courtesy of CeramiSphere Ltd.].

**Scheme 3. Microparticles Synthesis Flow-Chart from O/W Emulsions**



This approach enables incorporation into a preparation of a high load of ingredients (even 90% of the weight of the

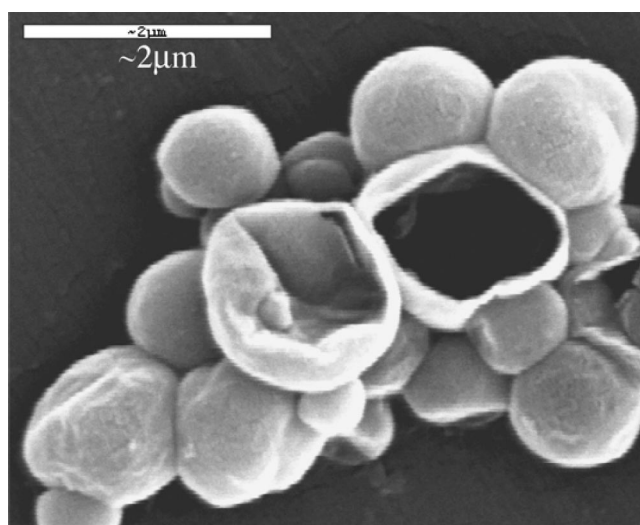


**Figure 16.** Representative SEM micrographs of microcapsules doped with the UV filter OMC, in which a rare open (broken) microcapsule is visible [Reproduced from ref 50 with permission].

particles) and thus achievement of sustained delivery of the active ingredients under defined mechanical or chemical conditions.

For example, the natural colorant  $\beta$ -carotene can be easily encapsulated in  $\text{SiO}_2$  microspheres by mixing the colorant (1.2 g) in TEOS (31.8 g). The organic phase is emulsified in 200 g of aqueous solution containing 1% cetyltrimethyl ammonium chloride (CTAC) with fast stirring (19 000 rpm) with an homogenizer and with the reaction vessel immersed in an ice–water bath for cooling. The resulting emulsion is then poured in 200 g of aqueous solution at pH 11.3 (NaOH) and stirred (400 rpm) at room temperature for 24 h, followed by stirring at 50 °C for 3 h. The product is washed, isolated, and freeze-dried to give a bright orange fine silica powder that, suspended in hydrophilic phases such as water, does not leach the encapsulated carotene, not even after prolonged heating of the aqueous suspension to 90 °C.<sup>32</sup> Also, in the case of the O/W approach, the technology for modular construction of the capsule shell affords control of the size and microstructure, with release rates ranging from non-leachable capsules to precisely timed release.

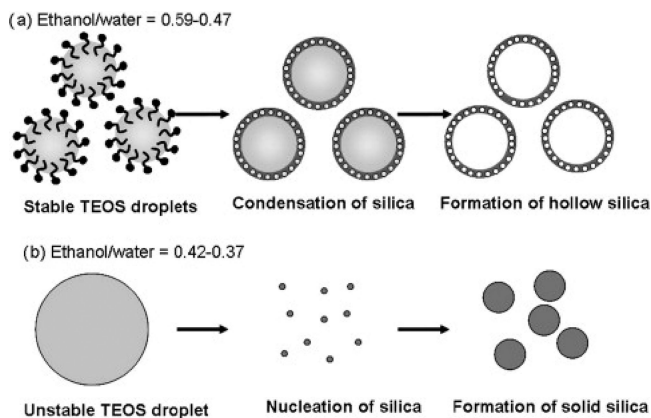


**Figure 17.** Schematic illustration of the formation processes of hollow and solid mesoporous silica spheres [Reproduced from ref 35 with permission].

### 2.2.1. Uniform Particles from O/W Emulsions

The uniformity of the size and shell thickness of the hollow silica spheres prepared by the O/W emulsion method is often poor due to the dynamic character of the emulsion droplets. It is remarkable, thus, to notice that the synthesis of highly uniform core-shell silica microcapsules simply requires the use of an alcohol such as ethanol in the oil-in-water emulsion. The approach was first suggested by Qi and co-workers for the synthesis of hollow shells of mesoporous silica in mixed water-ethanol solution using cetyltrimethylammonium bromide as the template.<sup>34</sup> More recently, Yang and collaborators have studied in detail the effects of the water-to-ethanol volume ratio and the content of TEOS and CTAB on the final morphology of the mesoporous silica microparticles.<sup>35</sup>

The mixture of water and ethanol helps to improve the stability of the oil droplets and thus the monodispersity of the resulting hollow silica spheres compared to the conventional oil-in-water emulsion approach. For example, hollow silica spheres with huge surface areas (924–1766 m<sup>2</sup> g<sup>-1</sup>) and pore sizes around 3.1 nm can be synthesized by carrying out the sol-gel ammonia-catalyzed polycondensation of oil droplets of TEOS stabilized by cetyltrimethylammonium bromide (CTAB) at the oil-water/ethanol interface (Figure 17).

The diameters of the hollow spheres can be tuned in the range from 210 to 720 nm by varying the ethanol-to-water ratio, whereas the shell thickness can be tailored by changing the concentration of CTAB (Figure 18). For example, the shell thickness of the silica spheres increases from 40 to 140 nm when the concentration of CTAB increases from 5 to 10 mM. At appropriate CTAB concentrations, the oil droplets are relatively stable and the silica can be deposited at the oil-water/ethanol interface, whereas too high concentrations of the surfactant will accelerate the hydrolysis of TEOS and reduce the stability of the oil droplets.

TEM observations indicate that the spheres are hollow with the shell made of mesoporous silica of thickness of about 40 nm (Figure 19b). The amount of ethanol introduced into the emulsion system must be optimized since EtOH can not only stabilize but also dissolve the TEOS droplets. When the content of ethanol introduced is not enough to ensure the stability of the oil droplets, full silica spheres are obtained as unstable TEOS droplets in the emulsion break up, giving rise to the formation of solid silica.

In the ethanol-to-water volume ratio 0.59–0.37 range, hollow microspheres are obtained. In detail, the diameter of

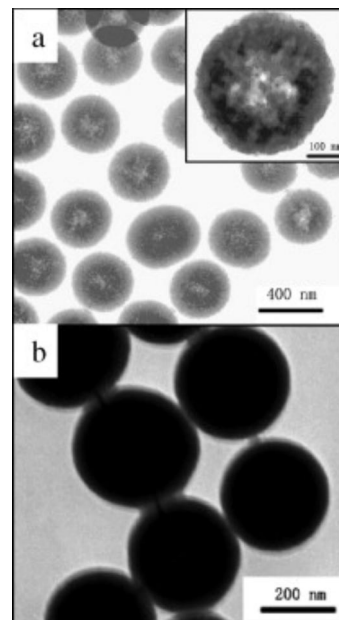


**Figure 18.** TEM images of mesoporous silica spheres obtained at (a) a CTAB concentration of 10 mM and (b) a CTAB concentration of 15 mM while the ethanol-to-water volume ratio was fixed at 0.59. The inset of part a shows a higher magnification of the hollow silica spheres [Reproduced from ref 35 with permission].

the spheres *decreases* with decreasing the EtOH/H<sub>2</sub>O ratio: from 720 nm when the volume ratio of ethanol-to-water is 0.59 (Figure 19a) to 350 nm when the ratio is decreased to 0.53 (Figure 19c), down to 150 nm when the ratio is decreased to 0.37 (Figure 19h).

When the ethanol-to-water ratio used is higher than 0.7 or lower than 0.37, full, solid spherical spheres are formed, pointing to the crucial role exercised by the ratio of ethanol/water used in the emulsion system. Indeed, Figure 20 shows that the autocorrelation functions ( $C(t)$ ) of the mixtures under different ethanol-to-water ratios are smooth for the reaction mixtures with EtOH/H<sub>2</sub>O = 0.59, 0.53, and 0.47, indicating good stability of the oil droplets.

Yet, the curves of the mixtures with ethanol-to-water ratios of 0.42 and 0.37 fluctuated, implying poor stability of the emulsion droplets, with a small fluctuation for the curve with the ethanol-to-water ratio of 0.47 reflected in the lesser uniformity of the hollow mesoporous silica spheres (see Figure 19e).

### 2.2.2. Microparticles from Emulsions with no Surfactant

By using the two-step sol-gel process (acid-catalyzed hydrolysis and base-catalyzed condensation) in an emulsified mixture, doped silica microspheres can be synthesized *without* the use of a surfactant, from what actually is a W/O emulsion.<sup>36</sup> Specifically, TEOS is first mixed with aqueous HCl in an acid catalyzed sol to which drugs are added for encapsulation.

After hydrolysis, aqueous base (NH<sub>4</sub>OH) is added and the resulting mixture (typically, 5 mL) is applied dropwise onto 100 mL of vegetable oil, stirring at speeds between 220 and 880 rpm. After about 1 h, microspheres with the typical large size of microspheres from W/O emulsions (ranges of 100–300 μm and 10–40 μm in diameter) were obtained whose compact surface morphology (Figure 21) is widely different from the irregularly shaped surface of xerogel granules of angular geometry and with multiple cracks.

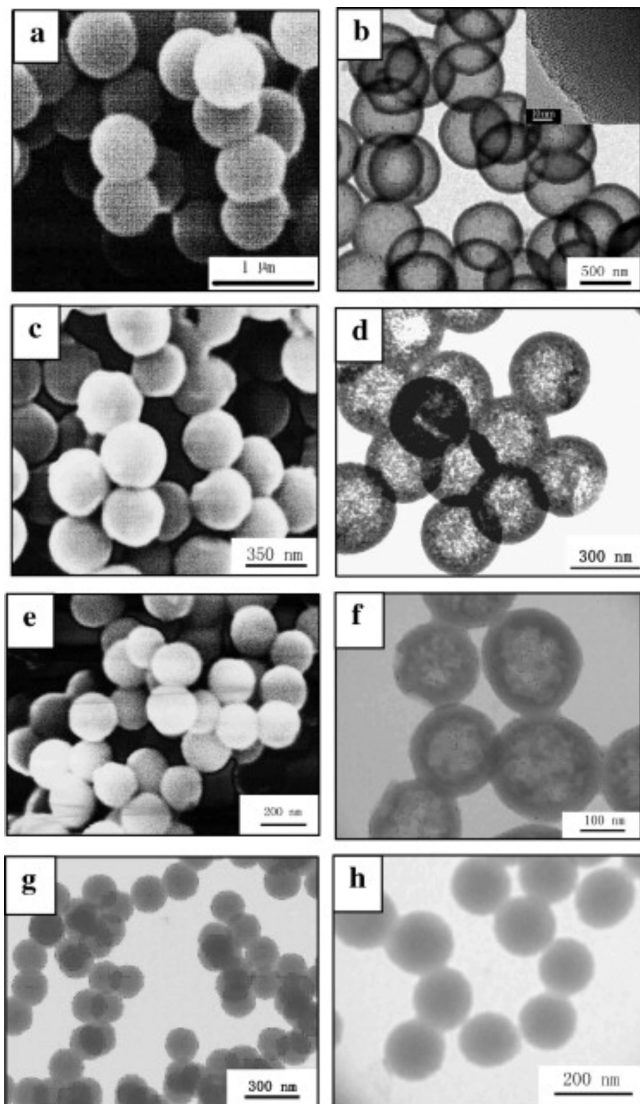


**Figure 19.** SEM images of mesoporous silica spheres synthesized with ethanol-to-water volume ratios of (a) 0.59, (c) 0.53, and (e) 0.47; TEM (b, d, f, g, and h) images of mesoporous silica spheres obtained at ethanol-to-water volume ratios of (b) 0.59, (d) 0.53, (f) 0.47, (g) 0.42, and (h) 0.37. The inset of part b gives the TEM image of the shell of a hollow sphere [Reproduced from ref 35 with permission].

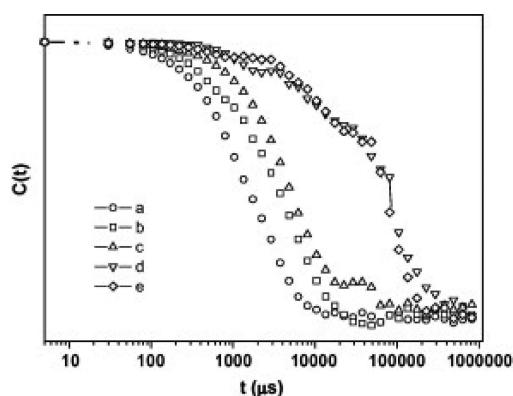


**Figure 20.** Curves of autocorrelation function ( $C(t)$ ) from dynamic light scattering measurements employed to evaluate the stability of the oil droplets in the reaction mixtures, varying with the time delay ( $t$ ) under ethanol-to-water volume ratios of (a) 0.59, (b) 0.53, (c) 0.47, (d) 0.42, and (e) 0.37 [Reproduced from ref 35 with permission].

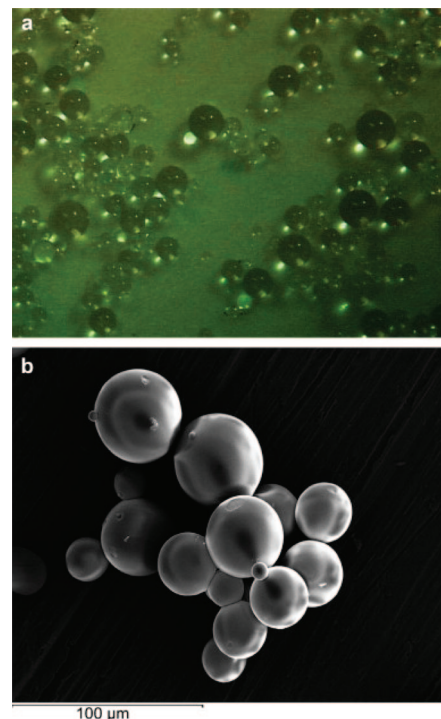


**Figure 21.** Optical and SEM micrographs of emulsified acid–base catalyzed silica microspheres. The optical (original magnification: 60 $\times$ ) and SEM (original magnification 600 $\times$ ) images show the appearance of microspheres in the size range of 100–300 and 10–40  $\mu\text{m}$  in diameter, respectively [Reproduced from ref 36 with permission].

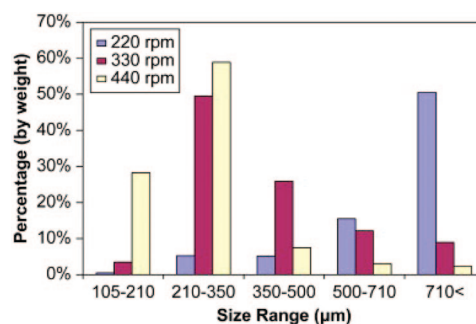


**Figure 22.** Size distribution of drug-free microspheres produced at various stirring speeds, as measured by sieving. The fraction dimensions are  $\mu\text{m}$ . With increase of stirring speed, the size of microspheres decreased. At 440 rpm, about 30% of the microspheres was in the size range 100–210  $\mu\text{m}$  [Reproduced from ref 36 with permission].

Again, the size of the microspheres is mainly dependent on the speed of stirring during emulsification (Figure 22). When the speed of stirring is increased, the size of the microspheres decreases and no nonspherical particles were obtained. Hence, at a stirring speed of 880 rpm, most of microspheres were in the size range of 10–40  $\mu\text{m}$ , whereas at 660 rpm most microspheres are below 100  $\mu\text{m}$ . At low speeds (around 220 rpm), about 50% of spheres are greater than 710  $\mu\text{m}$  and nonspherical particulates precipitate along with the microspheres.

Then, at 330 rpm, about 50% of the microspheres are in the range of 210–350  $\mu\text{m}$ , whereas, at 440 rpm, the percentage of the microspheres in this size range increases to about 60%, with the percentage of microspheres in the size range of 105–210  $\mu\text{m}$  also increasing to 28% (in contrast to less than 4% when the emulsification speed was 330 rpm).

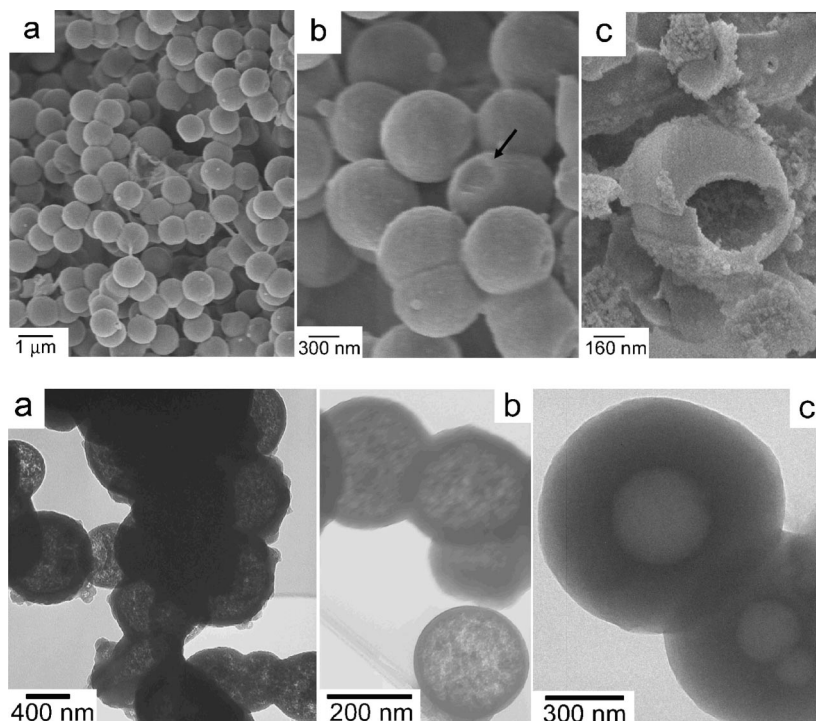


**Figure 23.** SEM images of monodisperse organosilica microcapsules (*top*) and TEM images of organosilica microcapsules containing the oil DEET (*bottom*) [Reproduced from ref 37 with permission].

The complementary approach avoiding the use of surface active agents, this time in O/W emulsion, is based on the self-catalytic sol–gel reaction of organosilanes at an oil/water interface. Hence, monodisperse organosilica microcapsules doped with the volatile repellent *N,N*-diethyl-*m*-toluamide (DEET) oil were prepared by Xin and co-workers in one step only without any surfactant or mediating reagent.<sup>37</sup> A typical synthesis procedure started from a mixture of 1 mL of methyltrimethoxysilane (MTMS) and 1 mL of DEET. The mixture was dropped into the mixture of water (50 mL) and 3-aminopropyltrimethoxysilane (ATMS, 0.5 mL). After stirring for 6 h at room temperature at 1000 rpm, a white microspheres dispersion was obtained. On average, the capsules were 900 nm in diameter and around 70 nm in shell thickness.

The SEM images of the organosilica capsules (Figure 23, *top*) clearly show monodisperse spheres about 900 nm in diameter. Figure 23c shows a crashed capsule, a relatively smooth outer surface, and an inner face with many granules. The TEM images (Figure 23, *bottom*) display the dark shells and the light cores of the capsules.

ATMS catalyzes the sol–gel process, as when MTMS or ATMS alone was added into water, there was not gelling even after 24 h of stirring. When both MTMS and ATMS are added in one pot, the gelling reaction occurred quickly and the solution changed into a white dispersion.

The TG curves of pure organosilica spheres  $\text{SiO}_{1.5}\text{R}_{0.5}$  and organosilica capsules  $\text{DEET}@ \text{SiO}_{1.5}\text{R}_{0.5}$  in Figure 24 show that in the former case the weight of solid spheres was kept constant between 100 and 250 °C, while the capsules lost 33 wt % in the same temperature range, pointing to evaporation of DEET from the capsules. By assuming the organosilica density as 2.0 g/cm<sup>3</sup>, this DEET content agreed well with the shell scale (about 1/6 of the capsule radius), enabling calculation of a relatively low 55% entrapment efficiency of DEET due to partial solubility of oil DEET in water as well as to further losses during drying.

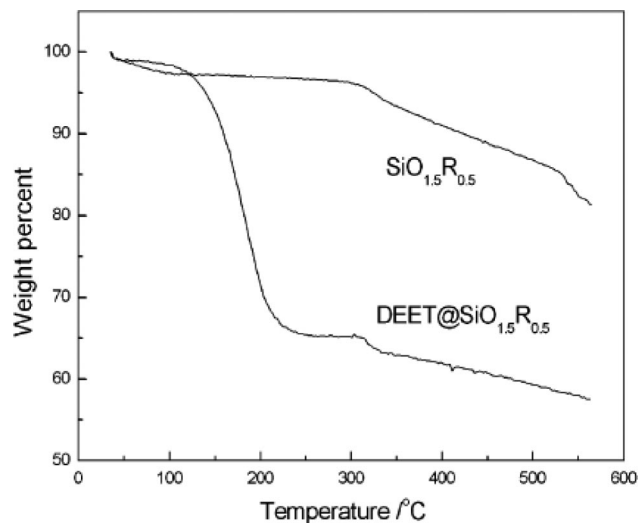


**Figure 24.** TG curves of organosilica solid spheres ( $\text{SiO}_{1.5}\text{R}_{0.5}$ ) and corresponding microcapsules ( $\text{DEET}@ \text{SiO}_{1.5}\text{R}_{0.5}$ ) [Reproduced from ref 37 with permission].

The concept of self-catalysis using a basic monomer such as aminopropyltrimethoxysilane is general and had previously been applied by Ottenbrite and co-workers to O/W synthesis of several hybrid ORMOSIL microparticles mediated by a surfactant.<sup>38</sup> Using comonomers of the type  $\text{R}'\text{-Si}(\text{OR})_3$ , where  $\text{R}' = \text{Me}$ , vinyl, allyl, or other hydrophobic groups, microarticles ranging from 100 to 500 nm in which up to 10 mol % of APS is incorporated into the siloxane particle network were obtained. The hydrophilic amino groups are located mainly on the particles surface due to the interfacial growth mechanism in the hydrophilic aqueous system. These capsules can also be used to encapsulate any kind of hydrophobic molecules in one step at room temperature, whereas the entrapped oils may be released through the micropores in capsule walls or by mechanical crash of the walls.

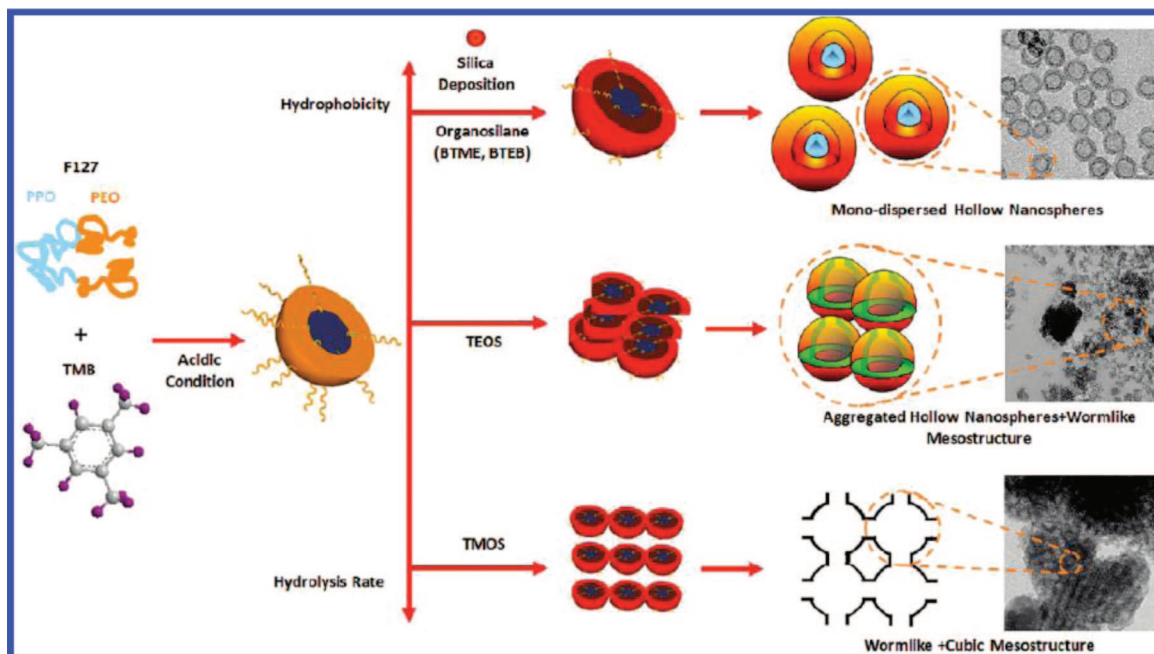


**Figure 25.** Formation mechanism of ORMOSIL nanoparticles and the relation between the morphology and the silane precursors [Reproduced from ref 39 with permission].

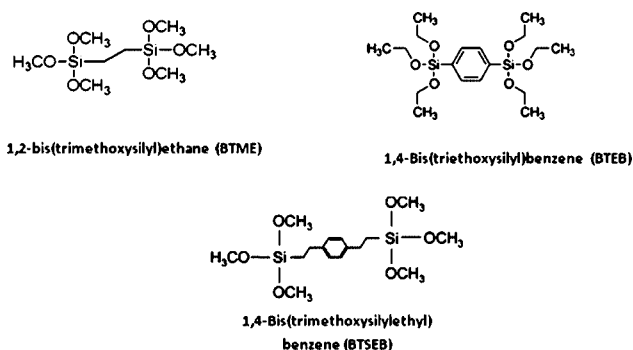


**Figure 26.** Siloxane and silsesquioxane precursors used for ORMOSIL nanoparticle synthesis in ref 39.

### 2.2.3. ORMOSIL Nanoparticles from O/W Emulsions

The versatility of the O/W approach was further demonstrated by the recent synthesis of organosilica hollow particles with large and flexible bridging organic groups reported by Yang and co-workers (Figure 25),<sup>39</sup> extending the surfactant-assisted approach to silsesquioxane nanoparticles from organotrialkoxysilanes in O/W microemulsion previously reported by Hay and Arkhireeva.<sup>40</sup>

Monodisperse particles of size around 25 nm were thus successfully prepared using precursors with ethylene, phenylene, and 1,4-diethylphenylene bridging groups in the network using Pluronic F127 block copolymer [(EO)<sub>106</sub>(PO)<sub>70</sub>(EO)<sub>106</sub>] micelles as a soft template under acidic conditions. In a typical synthesis, 1 g of F127, 1 g of 1,3,5-trimethylbenzene (TMB), and 5 g of KCl were dissolved in 60 mL of 2 M HCl at 40 °C under vigorous stirring. When the copolymer was fully dissolved, 10 mmol of organosilane precursor (Figure 26) was added under stirring. The resultant mixture was stirred at the same temperature for 24 h and aged at 100 °C for an additional 24 h. The solid product was recovered by filtration and air-dried at room temperature overnight. Finally, the residual surfactant was extracted by refluxing 1 g of the material in 200 mL of ethanol containing 1.5 g of concentrated HCl for 24 h.

As shown by Figure 25, the hydrophobicity/hydrophilicity of the silane precursor played an important role in the structure and morphology formation of the organosilicas. The hydrolysis and condensation rate in fact decreases in the sequence of TMOS > TEOS > BTME > BTEB. In any micelle-template sol–gel process, the rate of silica oxide formation depends on the availability of hydrolyzed silica species for the coassembly process between hydrolyzed silica species and the template. Hence, the employment of organosilane precursors with relatively low hydrolysis rates affords monodisperse hollow nanospheres. Instead, the use of fully hydrolyzable precursors such as TMOS and TEOS leads to the formation of mesostructured particles, since many more hydrolyzed silica species condense around the single micelles.

TEOS, with a slower hydrolysis rate than TMOS, tends to form the mixture of hollow nanospheres and mesostructured particles. The size of the ORMOSIL nanospheres could be enlarged by addition of a different amount of TMB, as the hydrophobic TMB molecules dissolve in the core (PPO block) of the micelle as a swelling agent to expand the micelle and help also the formation of monodisperse hollow nanospheres. Potassium chloride, in its turn, is used as it increases the tendency to form aggregated particles, suggesting that KCl increases the reactivity of the silane precursor to condense around the surfactant micelles.

First assembled in 1999 by Ozin using silsesquioxane precursors of the form (OEt)<sub>3</sub>Si–R–Si(OEt)<sub>3</sub>,<sup>41</sup> periodic mesoporous silicas (PMOs) have been thoroughly investigated, especially aiming to their employment as heterogeneous catalysts.<sup>42</sup> The fabrication of organosilica materials in nanospherical morphology is of even higher interest because of their potential applications in catalysis, drug delivery, and biochemistry.

### 2.3. Controlled Release

Release of the entrapped active(s) from both full micro-particles and core–shell microcapsules is enhanced compared

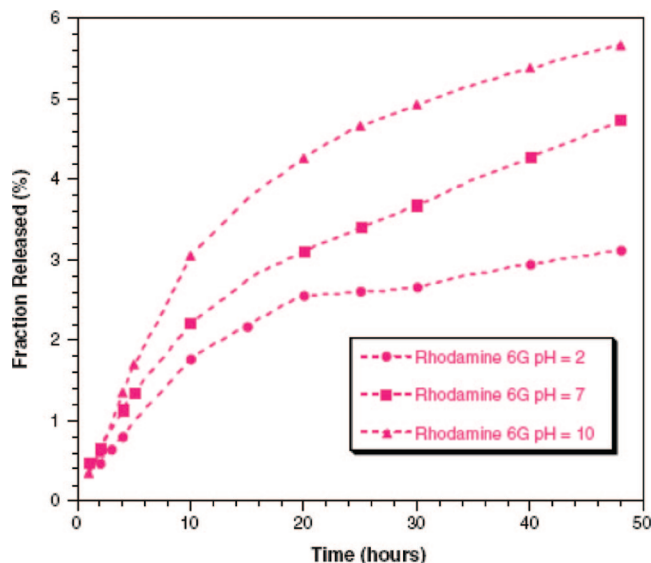


**Figure 27.** Influence of the synthesis pH on the release rate of Rhodamine 6G from microparticles of identical size [Reproduced from ref 16 with permission].

to leaching from xerogel particulate materials. In the former case, the shorter diffusion path accelerates by several orders of magnitude the release rate of the encapsulated molecules. As explained at length by Barbé,<sup>16</sup> this difference can be explained by the difference in diffusion length (15  $\mu\text{m}$  for the microparticles versus a few millimeters for the gels). In other words, the specific surface areas of the microsphere and monoliths synthesized under similar conditions are similar, but the proportion of active in contact with the external fluid (the diffusion front) in the smaller microspheres is much larger than that in the larger xerogel monoliths.

In the case of both full and hollow microspheres, the release rate is controlled by diffusion independently of particle size (10 nm–100  $\mu\text{m}$ ) and it is determined by the internal microstructure of the microparticles and thus by the initial sol–gel chemistry. Hence, the velocity of release can be varied from *mg/hours* to *mg/month* by changing parameters such as the water-to-alkoxide ratio, pH, alkoxide concentration, aging, drying time, and temperature (Figure 27).<sup>15</sup>

In general, increasing the hydrophobicity of the organo-silica matrix drastically reduces the release rate, as shown by Figure 28, profiling release for hydrophilic dyes entrapped in full microparticles obtained from W/O emulsions.<sup>15</sup> Clearly, with increasing amount of methyltrimethoxysilane (MTMS) in the TMOS/MTMS precursor sol, the release rate decreases. Remarkably, whereas the release from a xerogel of corresponding high hydrophobicity entirely stops, with microcapsules the release is still taking place, despite at a lower rate.

Also in the case of hollow  $\text{SiO}_2$  microspheres formed from W/O without surfactant, controlled and load dependent release is observed, which is remarkably different from that shown by similar sol–gel granules produced by grinding and sieving. In contrast to fast, short-term release from granules, the release from microspheres is slower and of longer duration (Figure 29).<sup>35</sup>

Ducheyne and co-workers ascribe this behavior, which is opposite to that observed from Barbé and co-workers for surfactant-assisted microparticle formation, to the reduction (by a factor of 2) of the values of surface area and the pore

volume compared to those of ground granules (Table 1). This reduces solution penetration into porous sol–gel particles and causes a corresponding reduction of the diffusion rates.

In addition, the degradation rate of microspheres is significantly slower than that of the granules; and it is also delayed due to differences in surface properties of the particles produced by emulsification (Figure 30). Whereas granules produced by casting and grinding have an irregular fractal geometry, the surface of the microspheres formed in contact with the emulsifying oil bath is that of smooth spheres.

As a result, whereas in the case of sol–gel granules the release profile can be modeled using a square root of time model for diffusion controlled release from a homogeneous porous matrix, the release from the silica microparticles is a diffusion controlled process whose release profile is best described by the Baker–Lonsdale model (eq 5) for diffusion from matrices of spherical shape.

$$\frac{3}{2} \left[ 1 - \left( 1 - \frac{M_1}{M_0} \right)^{2/3} \right] - \frac{M_1}{M_0} = kt \quad (5)$$

Finally, the nature of the dopant (the antibiotic vancomycin or analgesic bupivacaine) does *not* noticeably affect the dissolution rate (the  $k$  values for microspheres in eq 5 are independent of the specific drug incorporated; with vancomycin or bupivacaine, the  $k$  values were 0.018 and 0.019  $\text{h}^{-1}$ , respectively). Overall, the resulting delayed and sustained release represents an excellent profile suitable for preclinical studies currently underway.<sup>43</sup>

Sol–gel molecular entrapment is largely different from adsorption not only for xerogels but also in the case of microspheres. This is shown for example by the release profile of the water-soluble antibiotic gentamicin sulfate (GS) from silica hollow microspheres (Figure 31) obtained by direct sol–gel encapsulation in a W/O emulsion,<sup>44</sup> compared to release from GS-loaded hollow silica spheres<sup>45</sup> obtained by the immersion method.

Whereas the former system has a good drug release profile with rapid release of ca. 55% GS during the initial 2 h followed by a slower release rate (Figure 32), which allows a sustained concentration of the pharmaceutical, GS-loaded hollow silica spheres obtained by the immersion method release about 90% of the drug within 2 h, since most GS molecules are adsorbed at the microcapsules' outer surface.

The kinetics of the release of drug from porous carrier materials is a time-dependent process based on Fickian diffusion and has been described by Higuchi in the early 1960s as a square root time process.<sup>46</sup> According to this model, the dopant molecules are uniformly distributed throughout the matrix. The release percentage versus square root time profiles presented in Figure 33, however, shows that silica microcapsules entrapping the GS molecules give place to a two-step release, which is related to the effective encapsulation of drug molecules into the void cores of the silica microcapsules.

The drug molecules encapsulated in the inner cores of silica microcapsules can only diffuse through the pores in the shells. When the concentration of entrapped drugs in the confined space is halved, the diffusion driving force declines and so does the release rate.

In general, hollow mesoporous silica spheres have a high molecular storage capacity. However, the calcination step employed in the synthesis of uniform hollow spheres from

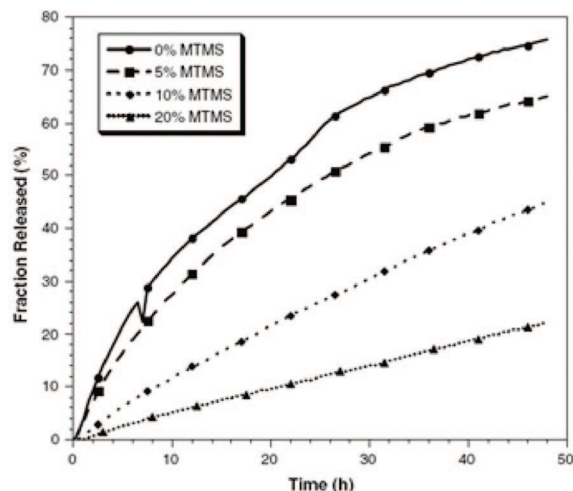
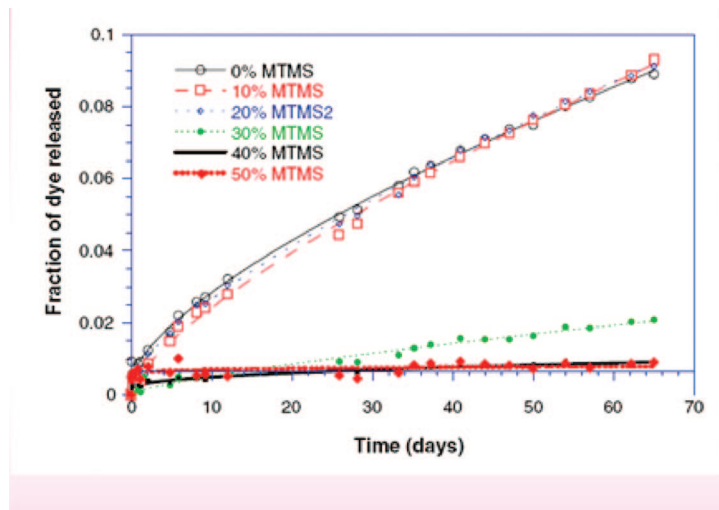


**Figure 28.** Release of Orange 2 in water from (left) xerogels synthesized with different amounts of MTMS; and (right) from microcapsules synthesized with different amounts of MTMS [Reproduced from ref 16 with permission].

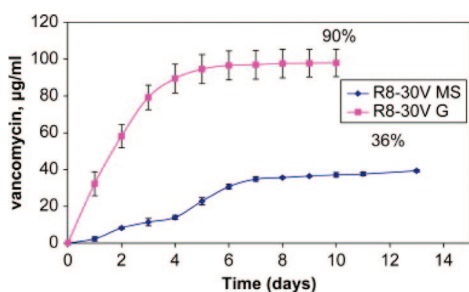


**Figure 29.** Cumulative vancomycin release ( $\mu\text{g/mL}$ ) from microspheres (MS) or ground granules (G) as a function of immersion time in PBS. Although the microspheres and granules were made from the same sols, the release profiles are largely different [Reproduced from ref 36 with permission].

**Table 1. Characteristics of Porosity of Acid-Base Catalyzed Sol Gel Granules and Emulsified Microspheres Including Surface Area (SA), Pore Volume (PV), Average Pore Diameter (PD), and Pore Diameter Distribution<sup>a</sup>** [Reproduced from Ref 36 with Permission]

material	SA, $\text{m}^2/\text{g}$	PV, $\text{cc/g}$	PD ave, nm	PD range, nm
microparticles	517	0.31	2.38	1.5–5
granules	283	0.18	2.55	1.5–7

<sup>a</sup> Composition of both granules and microspheres was similar (water/TEOS ratio of 8 and 30 mg/g vancomycin concentration).

W/O emulsions (section 2.1.1) prevents direct doping of the capsules during the sol–gel oxide formation. In this case, an elegant solution for controlled release has been demonstrated by Shi and co-workers using polyelectrolyte multilayers coated on the spheres by simple addition to a suspension of the hollow spheres.<sup>47</sup> Now the capsules can act as a switch for drug release which is controlled by the pH or ionic strength of the release medium (Figure 34).

The concept is general and is applicable to any water-soluble drugs with molecular size *smaller* than the pore diameter of the mesoporous silica spheres, as shown, for instance, by gentamicin molecules stored in hollow mesoporous silica spheres coated with polyelectrolyte multilayers.<sup>48</sup> When the pH value of the solution is lowered from 8 to 2, gentamicin molecules are rapidly released in solution due to the higher permeability of PAH/PSS multilayers, and release is complete after 30 h (Figure 35); in basic solution there practically is no release. By varying the pH value, true controlled release of the active ingredient can be achieved.

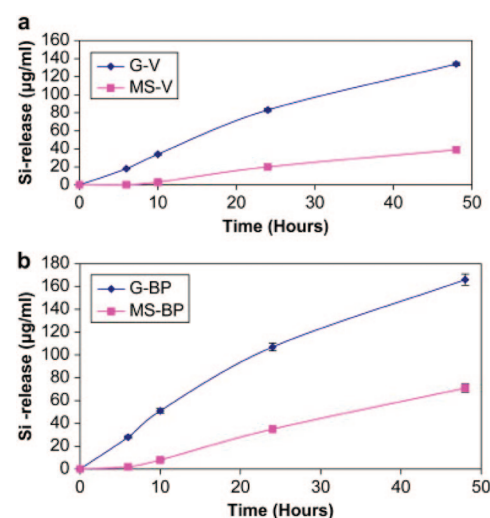


**Figure 30.** Dissolution profiles (measured as the cumulative Si-release versus immersion time in PBS) of acid–base catalyzed microspheres (MS) and ground granules (G) loaded with (a) vancomycin (V) or (b) bupivacaine (BP). The emulsified microspheres and ground granules were derived from the same sols ( $R$  equal to 8, 30 mg/g vancomycin or  $R$  equal to 6, 50 mg/g bupivacaine) [Reproduced from ref 36 with permission].

### 3. Applications

Porous sol–gel microparticles made of amorphous  $\text{SiO}_2$  are biocompatible and hydrophilic and thus can be easily suspended in water. Rapid biodegradability of silica microparticles is shown by fast dissolution in physiological buffers at pH 7.4 (in the open configuration, which closely models *in vivo* conditions).<sup>49</sup> Moreover, silica particles have high mechanical strength and thermal stability. The physical and chemical protection of the entrapped dopant from extreme acid or base, as well as from enzymatic degradation and from detergents, opens up applications in at least three major industrial sectors:

- *Healthcare* (delivery of poorly soluble drugs, gene therapy, wound healing)
- *Specialty Chemicals* (phase change materials for building applications, encapsulation, and release of reactive compounds such as bleach)
- *Cosmetics and food* (release of oil and flavors for cosmetic and food applications)

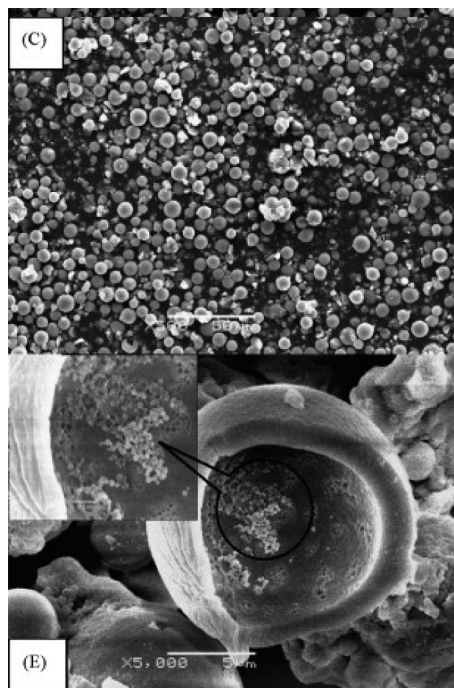


**Figure 31.** SEM images of silica microcapsules encapsulating gentamicin sulfate obtained from a W/O emulsion [Reproduced from ref 44 with permission].

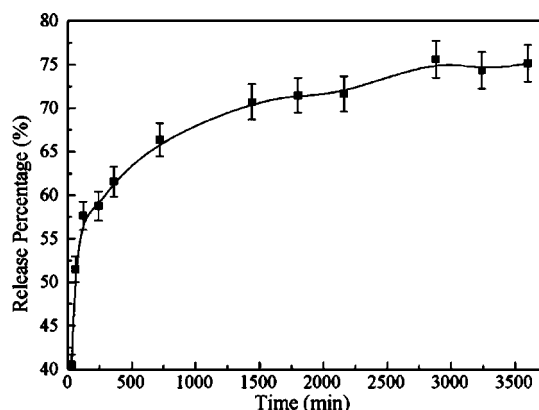


**Figure 32.** In vitro release profile of gentamicin sulfate entrapped in hollow silica microcapsules obtained from a W/O emulsion [Reproduced from ref 44 with permission].

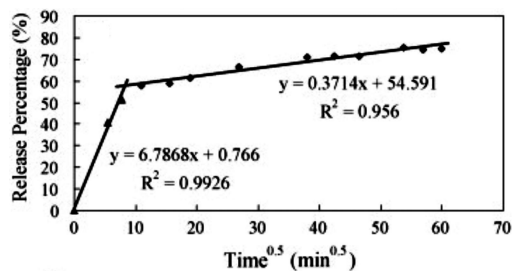


**Figure 33.** Release percentage vs square root time profiles for GS encapsulated in silica microcapsules [Reproduced from ref 44 with permission].

In general, doped silica microspheres will find applications as catalysts, dyes, inks, biomaterials, drug release capsules, and cosmetics. In the following, however, instead of covering all existing or forthcoming applications, we focus on a selection of technologies to demonstrate that silica micro-particles doped with active ingredients are indeed smart materials suitable for widely different end usages.

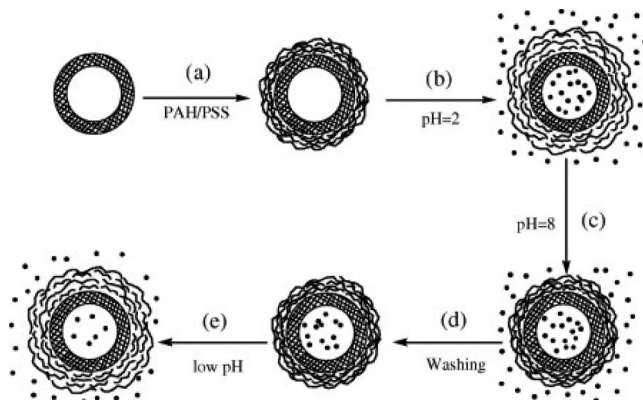


**Figure 34.** Polyelectrolyte multilayers (PEM), consisting of sodium polystyrene sulfonate (PSS) and poly(allylamine hydrochloride) (PAH) layers, coating on hollow mesoporous silica (HMS) spheres (step a), and pH-controlled storage (steps b, c, d) and release of drug molecules (step e) [Reproduced from ref 47 with permission].

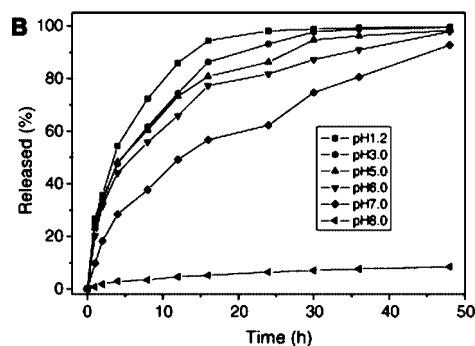
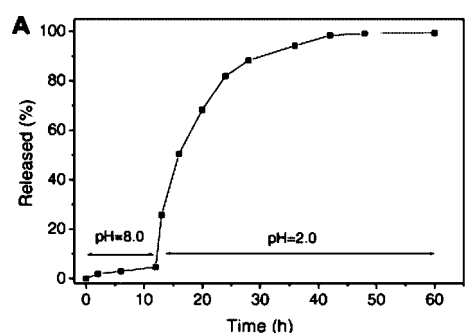


**Figure 35.** (A) pH-controlled release switching of gentamicin molecules from the  $G_{60}$ -PEM/HMS system and (B) the release processes of gentamicin molecules from the  $G_{60}$ -PEM/HMS system at different pH values in solutions [Reproduced from ref 48 with permission].

### 3.1. Advanced Sunscreens

Supplied as freely dispersed suspensions in water, hydrophilic silica microcapsules enhance the bioavailability of the entrapped active ingredients. Moreover, silica microcapsules from O/W emulsions are clear and smooth to the touch and are ideally suited for cosmetic formulations. Perhaps not surprisingly, therefore,  $\text{SiO}_2$  microcapsules doped with organic sunscreen molecules were the first large-scale commercial application of sol-gel doped microparticles.<sup>50</sup> Marketed in 2001 by Merck with the name *Eusolex UV-Pearls*, these suspensions are used to formulate high sun protection factor (SPF) lotions with improved safety profiles. Many of the molecules used as sunscreens, such as 4-methylbenzylidene camphor (4-MBC) and octyl methoxycin-

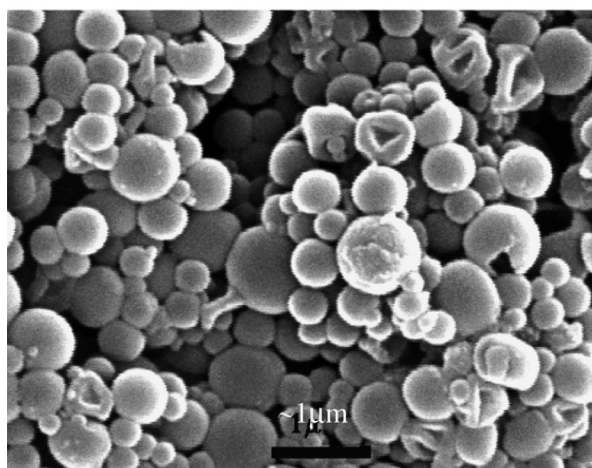
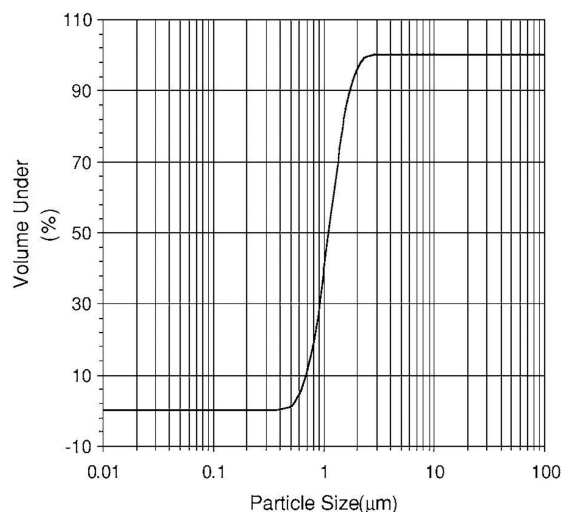


**Figure 36.** Particle size distribution (*top*) of microcapsules (*bottom*) obtained, represented as the volume percent of the particles from the total sample under a selected size [Reproduced from ref 50 with permission].

namate (OMC), in fact, show estrogenic activity and are potential endocrine disrupters.<sup>51</sup>

In a typical encapsulation procedure, the oil phase, composed of a sunscreen/TEOS mixture, is added under mixing to the water phase, containing a surfactant and a base catalyst, giving a molar ratio TEOS/absorber/water = 1/0.7/191. Silica microparticles comprised of a core–shell structure with a shell width of ca. 100 nm and a size with a narrow size distribution in the range 0.3–3  $\mu\text{m}$  are then obtained (Figure 36).

In detail, the product is supplied as an aqueous dispersion containing approximately 35% (w/w) of the UV absorber at pH between 3.8 and 4.2. The white liquids contain capsules of about 1.0  $\mu\text{m}$  diameter (on average), 90% of which are <2.5  $\mu\text{m}$  in diameter and, thus, sufficiently small to be transparent when applied to the skin and to give a pleasant feeling. Concerning penetration of the encapsulated sunscreens into the body, Figure 37, displaying the quantity of UV absorber extracted, shows that this is at least half reduced compared to penetration from nonencapsulated sunscreens. In practice, the encapsulated UV filters predominantly remain on the surface of the skin. In other words, the process yields particles small enough to give a pleasant nongritty feel yet large enough so as to avoid penetrating the epidermis.

In 2008 the Israeli company that developed the technology sold this sunscreen activity to Merck Serono,<sup>52</sup> and currently,

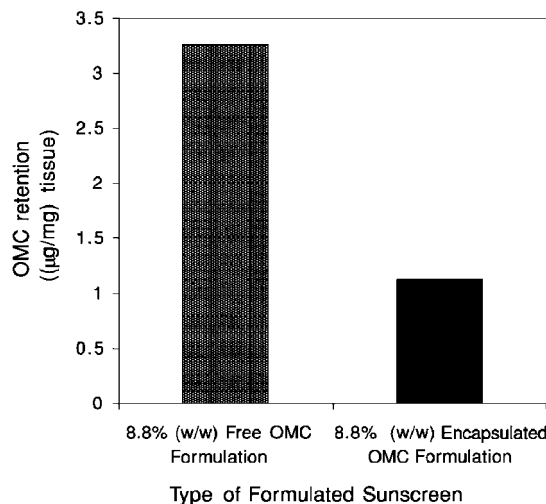
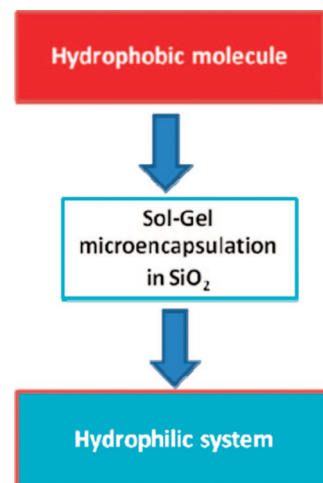


**Figure 37.** Human epidermal penetration studies of encapsulated octyl methoxycinnamate (OMC) vs free OMC [Reproduced from ref 50 with permission].

**Scheme 4.** Once Entrapped in Hydrophilic  $\text{SiO}_2$  Microparticles, Hydrophobic Organic Molecules Can Be Easily Formulated (Incorporated) into the Aqueous Phase



a number of commercial cosmetic preparations use *Eusolex UV-Pearls* as effective and safe sunscreens, providing the benefits of UVA and UVB filters while reducing undesired side effects due, for example, to photodegradation of the sunscreen molecules inducing free radicals formation and interaction with body tissues.

A general concept arising from this original application is that aqueous microemulsion dispersions provide new opportunities for cosmetic formulators. Hydrophobic, oil-soluble organic molecules can now be incorporated into the aqueous phase (Scheme 4), and incompatibilities between cosmetic ingredients can be prevented to the benefit of novel combinations in *one* cosmetic product.

### 3.2. Advanced Anti-Acne Therapy

More recently, the same approach has been extended by Sol–Gel Technologies Ltd. to microcapsules made of sol–gel entrapped benzoyl peroxide (BPO) for effective, nonirritating treatment of acne.<sup>53</sup> The inert  $\text{SiO}_2$  core shells now serve as a safe protective barrier, preventing direct contact between the BPO and the skin and significantly reducing side effects. In this case, the amount of skin lipids controls the rate at which the BPO is released, as the release

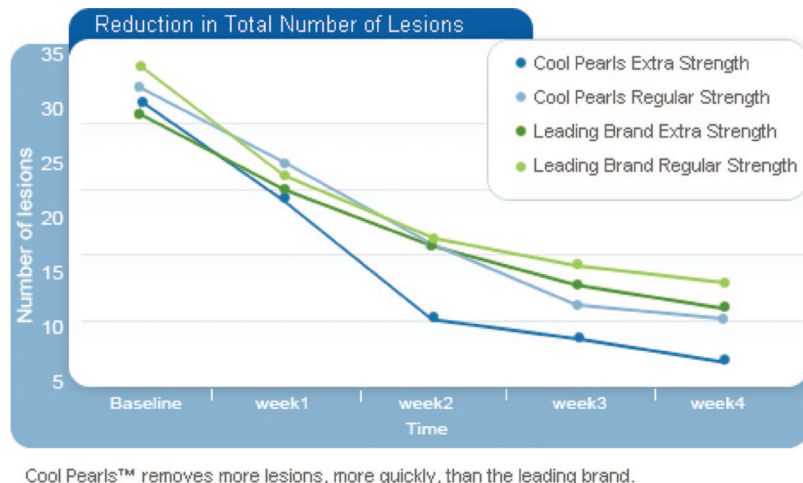


**Figure 38.** Reduction in the number of lesions among patients treating acne with *Cool Pearls BPO* and with competing, traditional BPO-based formulations (Source: Sol-Gel Technologies Ltd.) [Reproduced from [www.sol-gel.com](http://www.sol-gel.com), with permission].

mechanism involves migration of the skin's natural oily secretions through the silica pores into the capsule. The oils dissolve the BPO crystals and carry the dissolved BPO molecules to the sebaceous follicles.

In a clinical study (Figure 38), the product (*Cool Pearls BPO*) was tested and compared to the traditional market products, showing faster efficacy (visible reduction of acne in 3 days and substantially more effective with continued use) but avoiding the irritation, redness, and dryness caused by freely available BPO.

Transferred to an international dermatology products company in the U.S., the technology was first commercialized in late 2009 in two *Cool Pearls* anti-acne kits.

### 3.3. Long-Lasting Yeast

Living microorganism *Saccharomyces cerevisiae* (S.c.) yeast encapsulated in SiO<sub>2</sub> microparticles show both enhanced bioactivity and prolonged stability.<sup>54</sup> Yeast induces glucose fermentation, and its bioactivity is measured by the amount of CO<sub>2</sub> released from culture as a result of the (nonaero) fermentation of glucose (eq 6).



Mellati and co-workers synthesized two set of microcapsules (Figure 39) by mixing commercial yeast suspended in water with TMOS as silica precursor in a W/O emulsion. Vegetable oil was the organic phase, and the resulting emulsion was stirred at 600 rpm or at 1200 rpm.

Results show that production of CO<sub>2</sub> by encapsulated yeast increases by about 150% compared to that with free, nonentrapped yeast. Interestingly, smaller particles (with size decreased from 175 to 110 μm by increasing the mixer rate from 600 to 1200 rpm) show up to 30% enhanced bioactivity.

In detail, bioactivity measured on days 1, 14, 21, and 28 after microencapsulation shows that on day 1 the total amount of CO<sub>2</sub> released from free S.c. reached 6 g after 3 h against 14 g for encapsulated yeast (Figure 40). On days 14, 21, and 28, there was no evident change for free yeast whereas the amount of carbon dioxide released from the encapsulated yeast increased up to 16–17 g, for both sets of microparticles. Finally, after 28 days the total amount of CO<sub>2</sub> from bigger particles decreased to 12 g, but there was *no* change

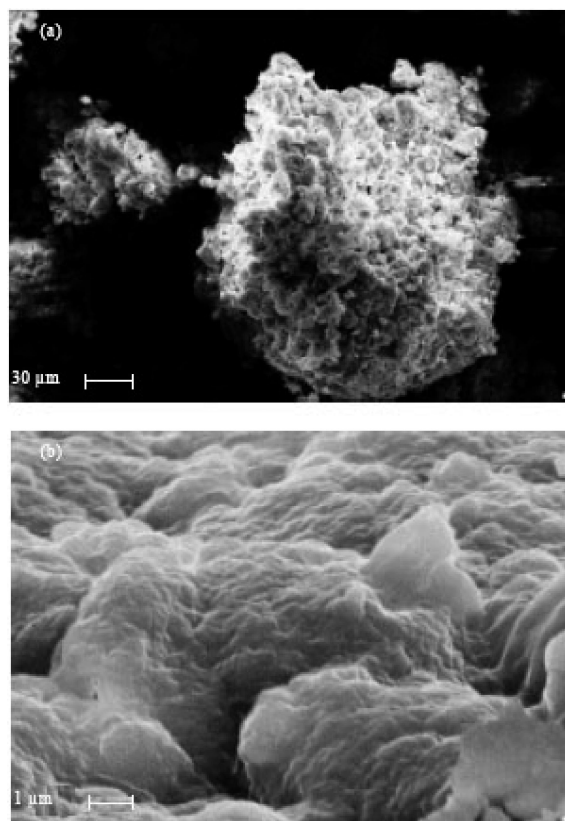


**Figure 39.** (a and b) Surface of the microcapsules captured using a SEM shows a microporous network which leads to mass transfer. Scale-bars represent 1 μm. [Reproduced from ref 54 with permission].

in bioactivity in the case of smaller particles, clearly pointing to enhanced stability of the smaller microsystem.

### 3.4. Enhanced Insulating Materials

Phase-change materials (PCMs) are important because they are latent heat storage materials suitable for the construction industry as low-energy alternatives to air-conditioning systems. In Europe only, air-conditioning consumes 15% of the total energy produced in one year.<sup>55</sup>

Paraffins such as *n*-octadecane melt in the comfortable room temperature range that lies between 20 and 26 °C, in the course of which they absorb massive amounts of latent

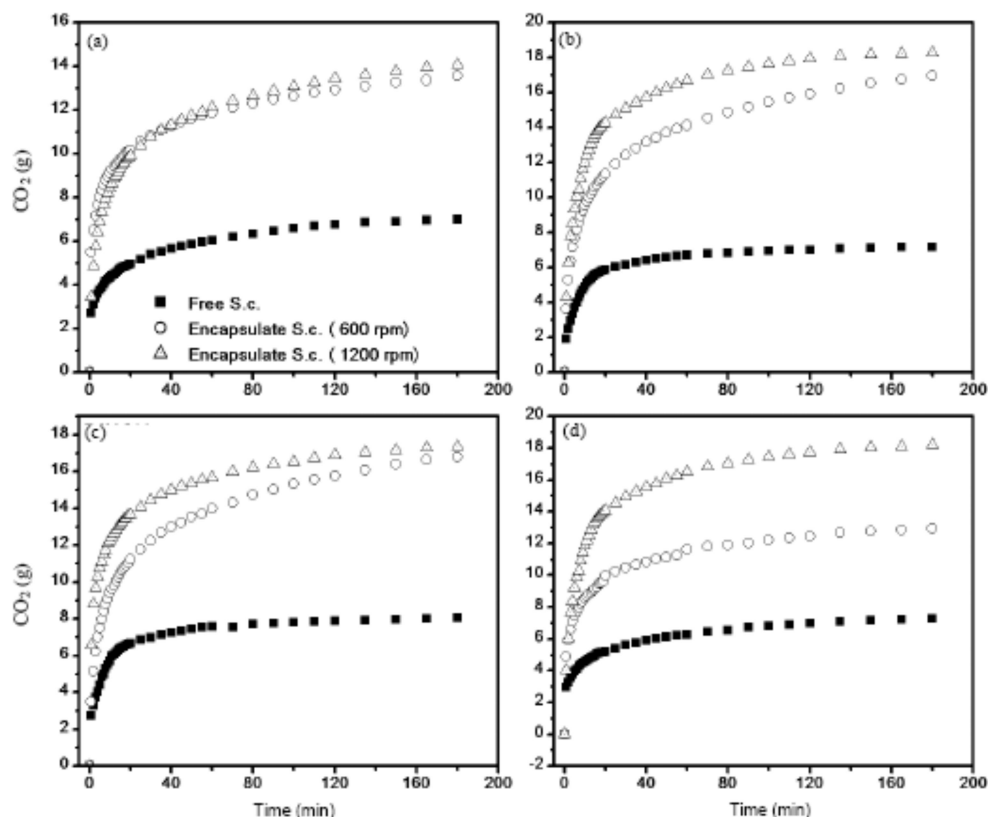


**Figure 40.** CO<sub>2</sub> release from free (■) S.c. and microencapsulated S.c. manufactured at 600 rpm (●) and at 1200 rpm (Δ): 1 day (a); 14 days (b); 21 days (c); 28 days (d) [Reproduced from ref 54 with permission].

heat from their environment and prevent the temperature from increasing. Microencapsulation here is crucial because it prevents wax leaching during the solid-to-liquid phase transition in tiny spheres, while the large surface areas and small volumes of the capsules mean that the heat can quickly be absorbed into the material and the cold rapidly released. At night, when the ambient temperature drops, the wax solidifies and the capsules release the heat they absorbed, making them ready to repeat the process the next day. Indeed, a material series made of wax entrapped into microcapsules of acrylic glass and integrated in conventional construction materials such as gypsum plaster is now commercialized by Basf with the *Micronal PCM* trademark.<sup>56</sup>

As shown by Zhang and co-workers, similar PCMs with enhanced thermal conductivity and phase-change performance can be successfully fabricated by microencapsulation of a wax such as *n*-octadecane in silica microspheres.<sup>57</sup> The best SiO<sub>2</sub> microcapsules are synthesized at pH 2.45 by using TEOS as silica source at *n*-octadecane/TEOS weight ratios of 60:40 and 50:50, respectively, ascribed to the fact that at the said pH value the condensation rate matches the self-assembly rate of the silica oligomers onto the surface of the *n*-octadecane micelles. The resulting particles exhibit (Figure 41g and h) a well-defined core–shell microstructure and uniform size of about 10 μm.

The synthesis of the microcapsules takes place only at 2.0 < pH < 3.0 but fails out of this range. Out of the above-mentioned range, the condensation rate is so fast that the silica oligomers do not have enough time to deposit onto the surface of the *n*-octadecane micelles, leading to a self-condensation of the silica precursors without effective encapsulation of the *n*-octadecane micelles.

At higher *n*-octadecane/TEOS weight ratio (70/30) and at pH 2.26, near the isoelectric point of silica, the condensation

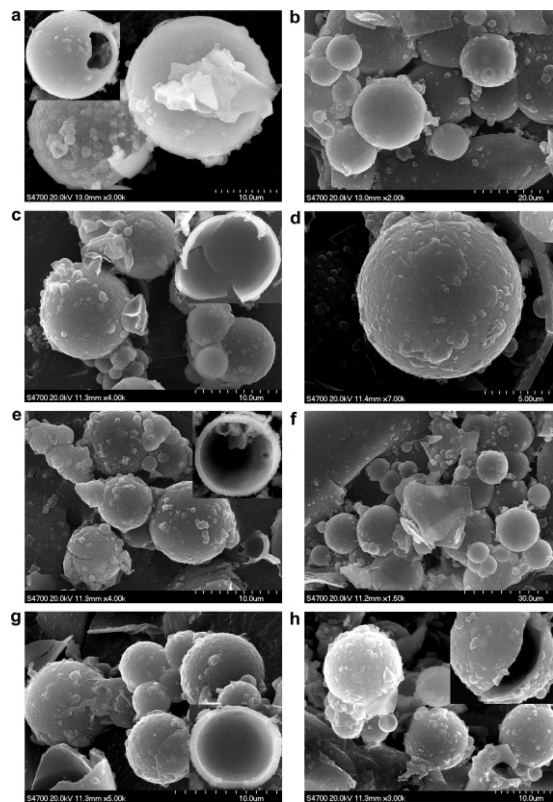


**Figure 41.** SEM images of the silica microcapsules synthesized at different *n*-octadecane/TEOS weight ratios and pH values: (a and b) 70/30 and pH 2.26; (c and d) 70/30 and pH 2.45; (e and f) 60/40 and pH 2.45; (g) 50/50 and pH 2.45; (h) 70/30 and pH 2.89; the inset is the image of the broken microcapsule obtained through milling [Reproduced from ref 57 with permission].

**Table 2.** Phase-Change Temperatures ( $T_m$  and  $T_c$ ) of the Silica-Microencapsulated *n*-Octadecane Synthesized under Different Conditions Obtained from the DSC [Reproduced from Ref 57 with Permission]

sample code	$T_c$ (°C)		$T_m$ (°C)	$\Delta H_c$ (J/g)	$\Delta H_m$ (J/g)	<i>n</i> -octadecane loading (wt %)	thermal conductivity (W m <sup>-1</sup> K <sup>-1</sup> )
	$\alpha$ -crystal	$\beta$ -crystal					
1	22.4	21.5	26.7	216.2	214.6		0.1505
2	23.0	20.7	26.6	131.5	130.7	64.7	0.3751
3	22.1	20.2	27.1	185.6	184.9	69.5	0.4568
4	22.5	20.7	27.2	146.3	142.6	61.2	0.5172
5	23.5	20.9	26.9	125.4	123.0	52.2	0.6213
6	23.3	21.6	27.1	142.2	140.9	66.2	0.3964

rate of the silica precursors is slow and a few silica oligomers deposit to form the shell, resulting in not uniform microcapsules with a thin silica shell with a rough surface (Figure 41a and b) that is easily cracked by vigorous agitation. The surface structure becomes finer as the acidity of the reaction solution decreases at pH 2.89, leading to faster silica condensation (Figure 39c–f) and thus to loose shells of low encapsulation efficiency, as also shown by the thermal behavior (see below).

The thermal conductivity of the microencapsulated *n*-octadecane is enhanced due to the presence of the high thermal conductive SiO<sub>2</sub> shell, whereas control of the dopant loading and acidity of the reaction solution enables control of the phase-change performance. The enthalpies involved in both melting and crystallization processes, indeed, are considerably reduced with increasing *n*-octadecane/TEOS encapsulation ratio (Table 2). In each case, encapsulation within the silica shell results in reduction of the  $T_m$  of the microencapsulated *n*-octadecane compared to that of the bulk wax, due to restricted freedom of the molecules of the entrapped wax molecules in the confined space of the capsules.

Both the encapsulation ratio and encapsulation efficiency are proportional to the *n*-octadecane/TEOS weight ratio that dominates the core material loading; however, they are also affected significantly by the acidity of the reaction solution.

For example, the encapsulation efficiency for the sample synthesized at an *n*-octadecane/TEOS weight ratio of 70/30 is low, as the microcapsules obtained at pH 2.26 are easily broken during the phase-change process due to their thin shells, which results in a leakage of *n*-octadecane inside the microcapsules after several cycles of the phase transition. However, when the microcapsules are synthesized at pH 2.45, the sample achieves a compact shell and the wax molecules are effectively encapsulated within the microcapsules without any leakage, pointing to concomitantly high encapsulation ratio and encapsulation efficiency.

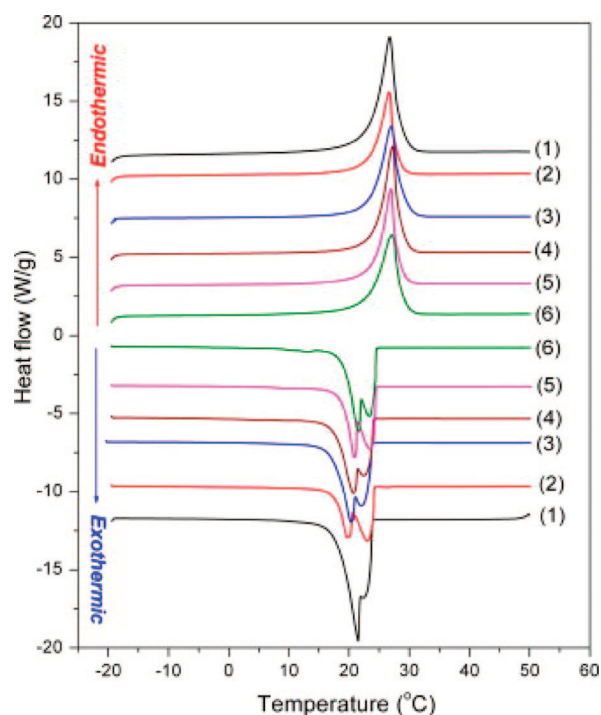
Thermograms of the bulk and silica-microencapsulated *n*-octadecane synthesized under different conditions (Figure 42) show the typical upward peak, indicating the endothermic process and the downward peak corresponding to the exothermic process.

The phase-change behavior of the microencapsulated *n*-octadecane in the cooling process differs from that of the bulk sample. Indeed, along with the well-defined exothermic peak at around 21 °C (attributed to the crystallization temperatures of the  $\beta$ -form crystals of *n*-octadecane), the  $\alpha$  peak (small shoulder at higher temperature) slightly shifts to a higher temperature while its intensity is enhanced. In other words, the inner silica wall acts as the nucleus in promoting the heterogeneously assisted phase transition and, thus, in an enhancement of the  $\alpha$ -form crystals, which leads to an improvement in the melting temperature and a widening of the temperature range for the phase transition.

### 3.5. Self-Healing Cement

Numerous chemical additives (admixtures) are commercialized by chemical manufacturers to improve the mechanical and chemical properties of concrete.<sup>58</sup> Among said additives, intense research efforts are focused on developing self-healing materials for crack-free cements, namely cement capable of self-repairing the cracks that form with time in cement, leading to degradation. A promising system indeed makes use of silica sol–gel microcapsules doped with polymerization catalyst.<sup>59</sup> Called by Shi and co-workers “passive smart microcapsules” (PSMs), the system is obtained by microencapsulation of a monomer healing agent (methylmethacrylate, MMA) and a polymerization catalyst (triethylborane, TEB) in two different sets of microcapsules. The capsules are synthesized from TEOS in a O/W emulsion in which self-assembly takes place at the acidic surface of sulfonated polystyrene particles.

In detail, the oil phase, either a 1 M MMA or TEB solution in hexane, was microencapsulated by dispersing 0.15 g of the sulfonated polystyrene particles (0.7  $\mu$ m in diameter) into 45 mL of water followed by introduction of 3 g of oil phase (oil/TEOS = 17/3 mol/mol) under continuous stirring at 500 rpm. After 24 h, microcapsules with oil core and silica shell were formed, with the polystyrene particles disentangled from

**Figure 42.** DSC thermograms of the bulk and microencapsulated *n*-octadecane synthesized under different conditions; the curve numbers correspond to the sample codes in Table 2 [Reproduced from ref 57 with permission].

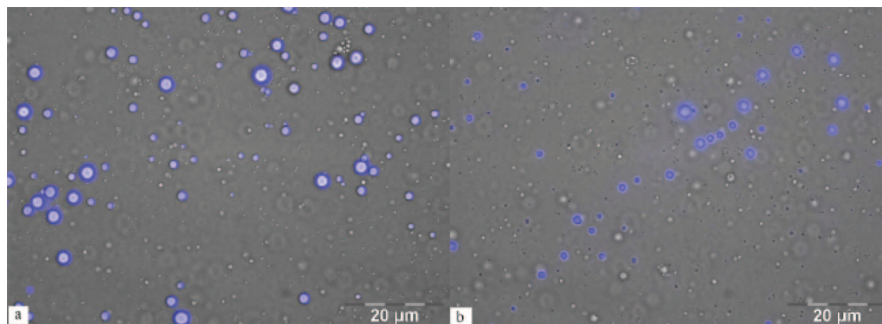


**Figure 43.** Optical microscopic images of (a) MMA healing-agent-containing microcapsules and (b) TEB catalyst-containing microcapsules [Reproduced from ref 59 with permission].

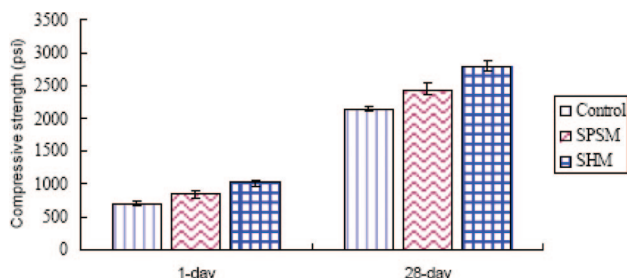


**Figure 44.** Compressive strength of three types of mortar specimens at 1-day and 28-day curing ages [Reproduced from ref 59 with permission].

the shell as shown by the microphotographs in Figure 43, which clearly indicates effective encapsulation of the oil phase including MMA or TEB (a fluorescent dye was used for the test) within the silica microcapsules.

The self-healing effect of the microcapsules dispersed in fresh cement mortar (along with carbon microfibers) is significant. For example, the self-healing mortars (SHMs) with passive smart microcapsules admixed showed higher compressive strength at both 1 day and 28 days, relative both to the control and to mortars modified with sulfonated polystyrene particles (SPSMs). In particular, the incorporation of PSMs increased the 1-day and 28-day compressive strength of the mortar by 45.8% and 30.4%, respectively (Figure 44).

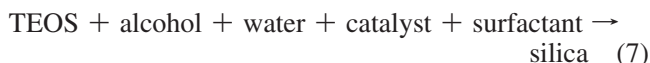
Self-healing is triggered by crack propagation through the microcapsules, which then releases the healing agent and the catalyst into the microcracks. The healing agent fills into the cracks by capillary action and, thus, by contact with the catalyst induces polymerization, bonding the cracked faces together (Figure 45).

Gas permeability of hydrated mortar samples at different ages also decreases, with a decrease in the permeability coefficient of 50.2% and 66.8% for the self-healing mortar (SHM) aged (cured) 3 and 30 days, respectively, relative to the control (Figure 46).

Sulfonated polystyrene microparticles do also reduce the permeability coefficient. Alas, in the case of SPSM, this reduction is significantly smaller with percentages of reduction of 23.8% and 24.0% after, respectively, 3 and 30 days. This indirectly shows that, for the self-healing mortar, the reduced permeability is mainly due to the self-healing effect of PSMs, which confers to cement mortar the ability to heal microcracks and, at least partially, to restore its mechanical properties.

#### 4. Economic and Environmental Considerations

In general, the ingredients of the typical sol–gel reaction for manufacturing silica-based microparticles are cheap and the capital investment required is relatively low. This is evident taking as reference the expanded Stöber process<sup>60</sup> (eq 7) employed both in the laboratory and in industry for the synthesis of uniform spherical silica particles by means of the room temperature hydrolysis of TEOS and subsequent condensation of silicic acid in alcoholic solutions (normally catalyzed by base):



In general, methoxysilicate TMOS reacts faster than ethoxysilicate TEOS because under both acidic and basic conditions the hydrolysis rate of TMOS is considerably higher than that of TEOS due to the retarding effect of the bulkier ethoxide group.<sup>61</sup> However, TEOS is much cheaper than TMOS and is the precursor actually employed by industry in practical applications.

Beyond low cost ethanol used as cosolvent, the price of TEOS is the main raw material cost. Today, the price of TEOS has dropped (it currently ranges from \$2 to \$6 per kg depending on grade and amount), as the global production of TEOS rose to a figure between 23,000 and 32,000 tons.<sup>18</sup> Beyond the cost of the small chemical plant where TEOS is stored and sol–gel processed under mild (i.e., low cost) conditions, the main cost of a sol–gel company is therefore that of labor. As typical of the nanochemistry business nature, the value of chemicals itself then becomes unimportant and all value creation resides in the application (Figure 47). In other words, almost all the value resides in the intellectual property behind the process affording the functional material.

As put by a leading industry practitioner,<sup>62</sup> this means that any nanomaterial manufacturing company, including sol–gel companies, must integrate itself *forward* within the value chain.

In 2006 a business report<sup>63</sup> estimated the overall value of the global market for sol–gel products at \$1 billion in 2006 and forecasted a relatively low annual growth rate of 6.3% from 2006 to 2011 (Figure 48).

Compared to the size of the global chemicals industry and to the potential applications of sol–gel functionalized sol–gel silicas, these figures are low. And the reason, we argue, lies in the relatively slow pace of innovation shown by most chemical companies in the 1990s. Prolonged low oil prices (averaging \$32 per barrel) simply rendered innovation not convenient.

Silica-based sol–gel products—developed at an advanced stage already during the 1980s—had to await the first decade

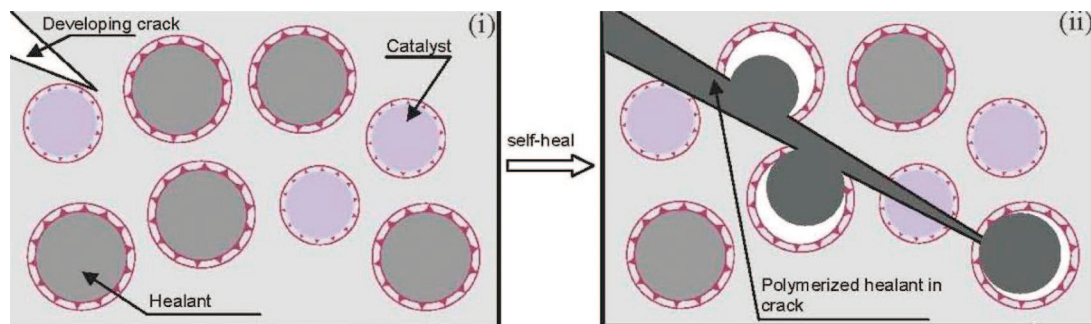


**Figure 45.** Schematic illustration of the self-healing concept in cement mortar: (i) healing agent and catalyst encapsulated in PSMs are dispersed in cementitious material and microcrack is forming; (ii) the crack ruptures the microcapsules and the healing agent contacts the catalyst, triggering polymerization that bonds the crack faces [Reproduced from ref 59 with permission].

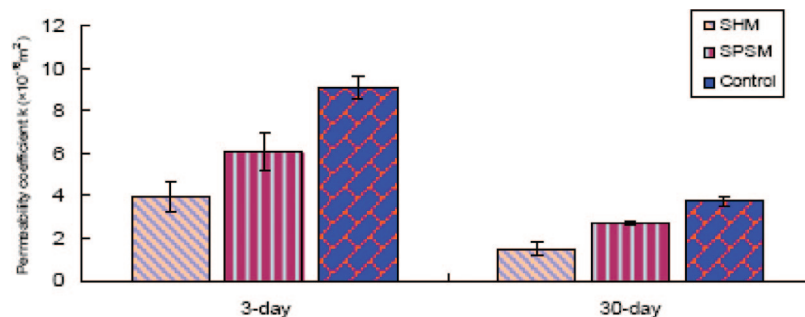


**Figure 46.** Permeability coefficients of cement mortar composite at 3-day and 30-day curing ages, after being loaded under 80% of compressive strength and subsequently set aside for 24 h [Reproduced from ref 59 with permission].

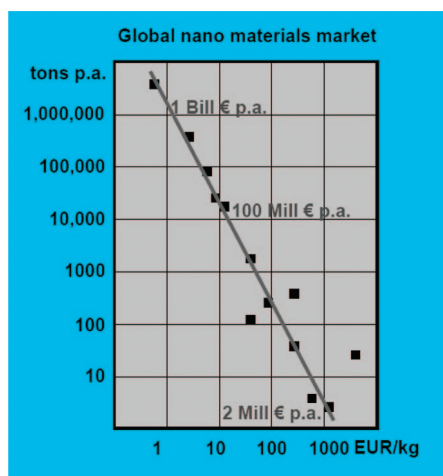


**Figure 47.** Despite the high price of nanomaterials, the small size of the market requires forward integration of the manufacturer within the value chain [Reproduced from ref 62 with permission].

of the years 2000s to reach the market. For example, the first water-based sol–gel formulations with an aqueous route replacing traditional Si alkoxide-based processes were reported in the early 1980s.<sup>64</sup> Yet we had to wait until 2007 to assist the launch of a new functional silica-based product from a large chemical company, when one could read on the Web pages dedicated to said product the following:

“Although sol–gel chemistry is known for decades now, examples of successful market introductions are limited. Furthermore almost all existing sol–gel treatments are solvent-based and consequently difficult to handle ... we offer today a broad variety of commercialized water-based products, which are also available in tons-scale.”<sup>65</sup>

Indeed, the concentration in many product segments of the chemical industry as a whole is very high, with a handful

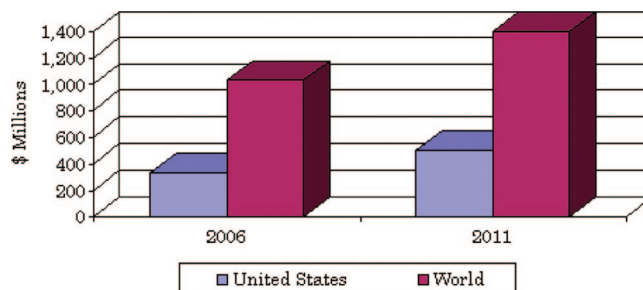


**Figure 48.** U.S. and world markets for sol–gel products in 2006 were forecasted to increase to \$1.4 billion by 2011 (Reproduced from ref 63 with permission).

of competitors often holding 80% of that segment. For example, in the U.S. the 50 largest companies generate about 70% of the revenue,<sup>66</sup> while the overall demand, being driven by the overall performance of many industry sectors, is intrinsically volatile (Figure 49).

In the early 2000s, the rapid increase of oil and natural gas prices along with the concomitant action of venture capitalists started to change the structure of the chemical business.<sup>67</sup> The price of energy and those of traditional raw materials (propene, for example) suddenly multiplied by a factor of 3 or more. Profitability in the chemical industry was again due to successful innovative products capable of creating a rapidly growing market, and the route to innovative chemical companies was open again.

The versatile sol–gel microencapsulation technology enables the production of new functionalized silica materials in which active, costly ingredients are protected (stabilized) and can be delivered where they are needed when needed in the needed amount, enhancing the precision and effectiveness of action. Perhaps not surprisingly, then, in the late 1990s both private and public venture capitalist funds, looking to invest in rapidly growing sectors, funded the first sol–gel

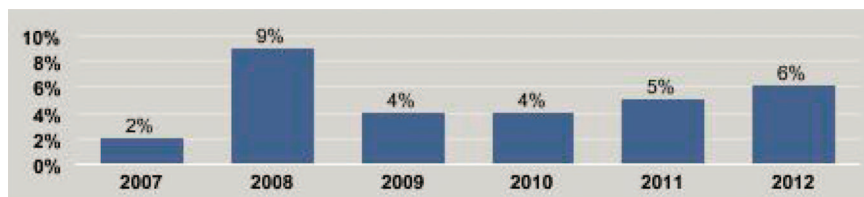


**Figure 49.** Forecast for chemical manufacturing growth in the U.S. (Reproduced from ref 66 with permission).

start-ups. This resulted in the rapid launch of several new products based on functionalized silicas,<sup>68</sup> including Sol–Gel Technologies Ltd. in Israel, where construction of the world’s first plant for the production of silica microcapsules had just been completed by a leading Europe’s chemical engineering company in 2001. Production started soon afterward, with all products being purchased by Merck for further integration into cosmetic formulations later sold to cosmetic companies. In 2009, then, Merck Serono opted for consolidating the production of *Eusolex UV-Pearls* in Germany,<sup>69</sup> where the low energy intensive sol–gel process can be profitably conducted despite the price of electricity in western Europe generally being 10 times higher than that in China (0.01 €/kWh in China versus 0.10 €/kWh in Europe).

From a manufacturing viewpoint, all waste of matter and energy is a cost which affects profitability, and thus, if economically and technically feasible, it should be eliminated because, in general, whatever the business:

$$\text{profits} = \text{revenues} - \text{cost} \quad (8)$$

$$\text{cost} = \text{cost}_{\text{intr.}} + \text{waste} \quad (9)$$

In this sense, the use of the “zero-waste” O/W emulsion approach to sol–gel microcapsules is preferable to processes carried out in W/O emulsions, in which large amounts of spent organic solvent (the oil) are (by)-produced. Indeed, it is of relevance here to notice that the sol–gel synthesis of surfactant-templated silicas was recently shown to be a *non*-eco-friendly process, mostly due to the use of non-biodegradable surfactants and organic solvent.<sup>18</sup>

Finally, the business benefits from the commercialization of functional sol–gel microcapsules will of course depend on the size and growth rate of their market. In the U.S. only, the acne therapy market is worth \$1 billion, and this gives an idea of the commercial value of the *Cool Pearls BPO* drug delivery technology. In the construction industry, where immense amounts of concrete are consumed annually, the employment of cheap silica-entrapped waxes as phase change materials will similarly be enormous,<sup>70</sup> with small additional costs incurred by the use of PCM sol–gel microcapsules to be recouped shortly and then provide free climate protection for many subsequent years.

## 5. Perspectives and Conclusions

In a recent insight paper<sup>71</sup> on the state and perspectives of nanochemistry, Ozin argued that nanoscience expectations were exaggerated, especially from a technological perspective and that the time has come for chemistry-enabled nanotechnology to afford new solutions to relevant problems. Now, even the most serious critics of environmentalism<sup>72</sup> agree that anthropogenic pollution is a serious issue and that sustainability is a major challenge facing humanity at this stage of our common evolution. We urgently need technologies capable of reducing the impact of our industrial and

living activities, including transportation, energy usage in buildings, and, in the chemical industry, green processes and green chemicals capable of replacing older hazardous chemical conversions and products.<sup>73</sup> Sol–gel functionalized materials may offer a solution to these and to many other related environmental and technical issues.

Some of us recently suggested<sup>22</sup> that the templating approach to silicates (in place of the traditional Stöber process) was likely to be one powerful driver leading to new relevant applications of doped silica gels. This assumption was based on the idea that by emulating natural designs, which combine hard and soft materials, one would get synergistic properties with useful functionalities.<sup>74</sup> Indeed, we propose here to call these materials “system materials” in the same sense for which in systems theory the properties of the system include and go beyond the properties of the parts comprising the system.<sup>75</sup>

The achievements selected in this account dealing with sol–gel microparticles show that this approach is eventually working, expanding the possibilities offered by traditional functional silica gels and offering solutions to some important problems in a number of fields as diverse as biotechnology, medicine, and energy saving. Research in the field is flourishing on a true international scale. A brief selection of the research Groups mentioned in this review shows that they operate in countries as distant as Australia, Japan, Israel, Hong Kong, the U.S., Iran, Malaysia, Germany, China, Korea, Canada, and France. In the meanwhile, many other research groups active in sol–gel research have expanded their activity to include sol–gel microparticles, and their efforts will be reflected soon in the scientific literature.

Only in the catalysis field of application, is it worth noting here that whereas periodic mesoporous organosilica (PMOs) applications to catalysis have been widely studied,<sup>76</sup> this is not the case for organosilica microparticles, despite the fact that McQuade<sup>77</sup> in the past decade has clearly shown the large potential of polymeric microcapsules in heterogeneous catalysis. Given the increasing relevance of heterogeneous catalysis in the fine chemicals industry,<sup>78</sup> we argue that hollow and full silica-based catalytic microparticles will soon become a hot topic in heterogeneous catalysis.<sup>79</sup>

In conclusion, one may notice the “green chemistry” principles developed since the mid-1990s concomitantly with advances in nanomaterials synthesis.<sup>80</sup> Indeed, as the current trend in commercial sol–gel nanotechnology continues, production of increasing quantities of sol–gel-derived silica-based nanomaterials will inevitably result in the introduction of these materials into the atmosphere, hydrosphere, and biosphere.<sup>81</sup> Basically, silica microspheres differ from silica xerogel particulate materials in their surface chemistry. Yet, they are readily biodegradable and of no toxicity. Thus, we argue in conclusion that sol–gel templated microspheres will actually emerge as one eminent class of those “instruments of sustainability”<sup>82</sup> invoked by Wiesner for a variety of chemistry-enabled nanotechnology applications.

## 6. Acknowledgments

This paper is dedicated to Palermo's Civic Hospital plastic surgeon Dr. Augusto Iaia for his remarkable intervention on D.P. in September 2008. We thank University of Southern Illinois's Professor Baul Dave for hosting one of us (M.S.) in his Lab since September 2009. Collaboration from Professor João Moura Bordado, of Lisboa's Instituto Superior Técnico, is gratefully acknowledged.

## 7. References

- Levy, D.; Reisfeld, R.; Avnir, D. *J. Phys. Chem.* **1984**, *88*, 5956.
- Avnir, D.; Coradin, T.; Lev, O.; Livage, J. *J. Mater. Chem.* **2006**, *16*, 1013.
- Avnir, D.; Blum, J.; Lev, O. Reactive Ceramic Nanocomposites with Organic and Bio-organic Dopants. In *Encyclopedia of Materials: Science and Technology*; Jurgen, K. H., Buschow, R. W., Cahn, M. C., Flemings, B., Ilshner, E., Kramer, J., Mahajan, S., Eds.; Elsevier Science: Amsterdam, 2001.
- Avnir, D. *Acc. Chem. Res.* **1995**, *28*, 328.
- Pagliaro, M. *Silica-Based Materials for Advanced Chemical Applications*; RSC Publishing: Cambridge, 2009.
- Pagliaro, M.; Ciriminna, R.; Wong Chi Man, M.; Campestri, S. *J. Phys. Chem. B* **2006**, *110*, 1976.
- Sanchez, C.; Julián, B.; Belleville, P.; Popall, M. *J. Mater. Chem.* **2005**, *15*, 3559.
- Gouin, S. *Trends Food Sci. Technol.* **2004**, *15*, 330.
- Kreimeyer, A. (BASF), "BASF keeps R&D spending at high level", press release, 28 January 2010.
- Microencapsulation: Methods and Industrial Applications*; Benita, S., Ed.; Informa Healthcare: London, 2005.
- Ghosh, S. K. Functional Coatings and Microencapsulation: A General Perspective. In *Functional Coatings*; Ghosh, S. K., Ed.; Wiley-VCH: Weinheim, Germany, 2006.
- McCoy, M. *Chem. Eng. News* **2008**, *86* (12), 26.
- van Driessche, I.; Hoste, S. Encapsulations Through the Sol-Gel Technique and their Applications in Functional Coatings. In *Functional Coatings*; Ghosh, S. K., Ed.; Wiley-VCH: Weinheim, 2006; Chapters 1 and 8.
- Lai, W.; Garino, J.; Ducheyne, P. *Biomaterials* **2002**, *23*, 213.
- Microemulsions: Properties and Applications*; Fanun, M., Ed.; CRC Press: Boca Raton, 2008.
- Barbé, C. J.; Kong, L.; Finnie, K. S.; Calleja, S.; Hanna, J. V.; Drabarek, E.; Cassidy, D. T.; Blackford, M. G. *J. Sol-Gel Sci. Technol.* **2008**, *46*, 393.
- Barbé, C.; Bartlett, J.; Kong, L.; Finnie, V.; Lin, H. Q.; Larkin, M.; Calleja, S.; Bush, A.; Calleja, G. *Adv. Mater.* **2004**, *16*, 1959.
- Backov, R. *Soft Matter* **2006**, *2*, 452.
- Arsenault, A.; Ozin, G. A. *Nanochemistry: A Chemical Approach to Nanomaterials*; RSC Publishing: Cambridge, 2005.
- Baccile, N.; Babonneau, F.; Thomas, B.; Coradin, T. *J. Mater. Chem.* **2009**, *19*, 8537.
- Pagliaro, M.; Ciriminna, R.; Palmisano, G. *Chem. Soc. Rev.* **2007**, *36*, 932.
- Ciriminna, R.; Palmisano, G.; Pagliaro, M. *Chem. Rec.* **2010**, *10*, 17. <http://www.ceramisphere.com.au>.
- Holmberg, K.; Jönsson, B.; Kronberg, B.; Lindman, B. *Surfactants and Polymers in Aqueous Solution*, 2nd ed.; Wiley: New York, 2002.
- Meixner, D. L.; Dyer, P. N. *J. Sol-Gel Sci. Technol.* **1999**, *14*, 223.
- Finnie, K. S.; Bartlett, J. R.; Barbe, C. J. A.; Kong, L. *Langmuir* **2007**, *23*, 3017.
- Brinker, C. J.; Drottning, W. D.; Scherer, G. W. A comparison between the densification kinetics of colloidal and polymeric silica gels. In *Better Ceramics Through Chemistry*; Brinker, C. J., Clark, D. E., Ulrich, D. R., Eds.; Materials Research Society: New York, 1984.
- Wang, J.-X.; Wang, Z.-H.; Chen, J.-F.; Yun, J. *Mater. Res. Bull.* **2008**, *43*, 3374.
- Singh, R. K.; Garg, A.; Bandyopadhyaya, R.; Mishra, B. K. *Colloids Surf., A: Physicochem. Eng. Aspects* **2007**, *310*, 39.
- Lee, M. H.; Oh, S. G.; Moon, S. K.; Bae, S. Y. *J. Colloid Interface Sci.* **2001**, *240*, 83.
- Fujiwara, M.; Shikawa, K.; Hayashi, K.; Morigaki, K.; Nakahara, Y. *J. Biomed. Mater. Res.* **2007**, *81A*, 103.
- Hideo, O.; Takahashi, K. *J. Chem. Eng. Jpn.* **1998**, *31*, 808.
- The original 2001 patent describing the technology is: Magdassi, S.; Avnir, D.; Seri-levy, A.; Lapidot, N.; Rottman, C.; Sorek, Y.; Gans, O. Method for the preparation of oxide microcapsules loaded with functional molecules and the products obtained thereof, US 6303149 (Granted to Sol-Gel Technologies Ltd.).
- Zhang, H.; Wu, J.; Zhou, L.; Zhang, D.; Qi, L. *Langmuir* **2007**, *23*, 1107.
- Teng, Z.; Han, Y.; Li, J.; Yan, F.; Yang, W. *Microporous Mesoporous Mater.* **2010**, *127*, 67.
- Radin, S.; Chen, T.; Ducheyne, P. *Biomaterials* **2009**, *30*, 850.
- Fei, B.; Lu, H.; Wang, R. H.; Xin, J. H. *Chem. Lett.* **2006**, *35*, 622.
- Ottenbrite, R. M.; Wall, J. S.; Siddiqui, J. A. *J. Am. Ceram. Soc.* **2004**, *83*, 3214.
- Liu, J.; Bai, S.; Zhong, H.; Li, C.; Yang, Q. *J. Phys. Chem. C* **2010**, *114*, 953.
- Arkhireeva, A.; Hay, J. N.; Oware, W. *J. Non-Cryst. Solids* **2005**, *351*, 1688.
- Asefa, T.; MacLachlan, M. J.; Coombs, N.; Ozin, G. A. *Nature* **1999**, *402*, 867.
- Yang, Q.; Liu, J.; Zhang, L.; Li, C. *J. Mater. Chem.* **2009**, *19*, 1945.
- In the Laboratories of Prof. P. Ducheyne at Pennsylvania University.
- Wang, J.-X.; Wang, Z.-H.; Chen, J.-F.; Yun, J. *Mater. Res. Bull.* **2008**, *43*, 3374.
- Zhu, Y. F.; Shi, J. L.; Li, Y. S.; Chen, H. R.; Shen, W. H.; Dong, X. P. *J. Mater. Res.* **2005**, *20*, 54.
- Higuchi, T. *J. Pharm. Sci.* **1963**, *52*, 1145.
- Zhu, Y.; Shi, J.; Shen, W.; Dong, X.; Feng, J.; Ruan, M.; Li, Y. *Angew. Chem., Int. Ed.* **2005**, *44*, 5083.
- Zhua, Y.; Shi, J. *Microporous Mesoporous Mater.* **2007**, *103*, 243.
- Finnie, K. S.; Waller, D. J.; Perret, F. L.; Krause-Heuer, A. M.; Lin, H. Q.; Hanna, J. V.; Barbé, C. J. *J. Sol-Gel Sci. Technol.* **2008**, *49*, 12.
- Lapidot, N.; Gans, O.; Biagini, F.; Sosonkin, L.; Rottman, C. *J. Sol-Gel Sci. Technol.* **2003**, *26*, 67.
- Schlumpf, M.; Cotton, B.; Conscience, M.; Haller, V.; Steinmann, B.; Lichtensteiger, W. *Environ. Health Perspect.* **2001**, *109*, 239.
- Weinreb, G. *Globes*, January 24, 2008.
- Cool Pearls Anti Acne Kits. See at the URL: [www.sol-gel.com/MainPage.aspx?id=133](http://www.sol-gel.com/MainPage.aspx?id=133).
- Mellati, A.; Attar, H.; Farahani, M. F. *Asian J. Biotechnol.* **2010**, *2*, 127.
- Pérez-Lombard, L.; Ortiz, J.; Pout, C. *Energy Build.* **2008**, *40*, 394.
- According to the company's information, a layer of PCM plaster approximately 1.5 cm thick has the same heat capacity as a concrete or brick wall, meaning that one can reap the benefits of lightweight design while still storing heat. They have been incorporated in numerous buildings, including the Haus der Gegenwart in Munich. See at the URL: [www.micronal.de](http://www.micronal.de).
- Zhang, H.; Wang, X.; Wu, D. *J. Colloid Interface Sci.* **2010**, *343*, 246.
- Sobolev, K.; Ferrada-Gutiérrez, M. *Am. Ceram. Soc. Bull.* **2005**, *11*, 16.
- Yang, Z.; Hollar, J.; He, X.; Shi, X. *Proc. SPIE* **2009**, *7493*, 74934L.
- Stöber, W.; Fink, A.; Bohn, E. *J. Colloid Interface Sci.* **1968**, *26*, 62.
- Brinker, C. J.; Scherer, G. W. *Sol-Gel Science: The Physics and Chemistry of Sol-Gel Processing*; Academic Press: New York, 1990.
- Hilarius, V. Farbe und Funktion—Von neuen Effekten zu innovativen Produkten; Merck KGaA: 2009. Available at the URL: <http://www.nanomat.de/pdf/hilarius.pdf>.
- BCC Research, *Sol-Gel Processing of Ceramics and Glass*; London, 2006.
- For an account on aqueous sol-gel routes of interest in biochemistry, see: Coiffier, A.; Coradin, T.; Roux, C.; Bouvet, O. M. M.; Livage, J. *J. Mater. Chem.* **2001**, *11*, 2039.
- Cited from [www.dynasilan.com](http://www.dynasilan.com).
- First Research Ltd. 2010. Data available at the URL: <http://www.firstresearch.com/industry-research/Chemical-ManufacturingIndustrial.html> (last time accessed, May 30, 2010).
- The Future of the Chemical Industry*; Jones, R., Ed.; American Chemical Society: Washington, DC, 2010.
- Remarkably, some of these venture funds were Government-owned, such as in the case of Canada's SiliCycle Inc.
- Chem. Eng. News, 2009, 87 (17), 15.
- For comparison, BASF claims annual cost savings of over 25,000 € using the more expensive acrylic glass entrapped wax as phase change material in a building in Germany. See at the URL: [www.micronal.de](http://www.micronal.de) (Last time accessed: May 27, 2010).
- Ozin, G. A.; Cademartiri, L. *Small* **2009**, *5*, 1240.
- Lomborg, B. *The Wall Street Journal*, November 2, 2006.
- Anastas, P.; Warner, J. *Green Chemistry: Theory and Practice*; Oxford University Press: Oxford, 2000.
- Wan, Y.; Zhao, D. *Chem. Rev.* **2007**, *107*, 2821.
- Anderson, P. W. *Science* **1972**, *177*, 393. For a recent account on the implications of systems theory for chemistry, see: Reiher, M. *Found. Chem.* **2003**, *5*, 23.
- Yang, Q.; Liu, J.; Zhang, L.; Li, C. *J. Mater. Chem.* **2009**, *19*, 1945.
- Broadwater, S. J.; Roth, S. L.; Price, K. E.; Kobašlija, M.; McQuade, D. T. *Org. Biomol. Chem.* **2005**, *3*, 2899.

- (78) *Catalysts for Fine Chemical Synthesis*; Roberts, S. M., Ed.; Wiley: New York, 2007.
- (79) A single report, dealing with core-satellite nanocomposite catalysts protected by a layer of mesoporous silica, shows that these composite structures are good recyclable catalysts: Ge, J.; Zhang, Q.; Zhang, T.; Yin, Y. *Angew. Chem., Int. Ed.* **2008**, *47*, 8924.
- (80) Dahl, J. A.; Maddux, B. L. S.; Hutchison, J. E. *Chem. Rev.* **2007**, *107*, 2228.
- (81) Murphy, C. J. *J. Mater. Chem.* **2008**, *18*, 2173.
- (82) Wiesner, M. R.; Lecoanet, H.; Cortalezzi, M. *Nanomaterials, Sustainability, and Risk Minimization*; IWA International Conference on Nano and Microparticles in Water and Wastewater Treatment, Zurich, Switzerland, 22–24 September 2003.

CR100161X